$^{40}Ar/^{39}Ar$ geochronology results for the Cave Canyon, Fountain Green North, Hilgard Mountain, Pine Park, Skinner Peaks, Tickville Spring, and Veyo quadrangles, Utah

by

New Mexico Geochronology Research Laboratory and Utah Geological Survey

2006

Utah Geological Survey Open-File Report 473

Utah Geological Survey
A division of
Utah Department of Natural Resources

Bibliographic citation for this data report:

New Mexico Geochronology Research Laboratory and Utah Geological Survey, 2006, $^{40}Ar/^{39}Ar$ Geochronology Results for the Cave Canyon, Fountain Green North, Hilgard Mountain, Pine Park, Skinner Peaks, Tickville Spring, and Veyo quadrangles, Utah: Utah Geological Survey Open-File Report 473, variously paginated.

This Open-File Report makes available raw analytical data from laboratory procedures completed to determine the age of rock samples collected during geologic mapping funded or partially supported by the Utah Geological Survey (UGS). The references listed in table 1 report the age of the samples and generally provide additional information such as the sample location, geologic setting, and significance or interpretation of the samples in the context of the area in which they were collected. This report was prepared by the New Mexico Geochronology Research Laboratory under contract to the UGS. These data are highly technical in nature and proper interpretation requires considerable training in the applicable geochronologic techniques.

Table 1. Sample numbers and locations.

Sample #	7.5' quadrangle	Latitude	Longitude	Reference
VY9503-1	Veyo	37° 21' 43.0"	113° 41' 13.0"	Hayden (in prep.)
VY9303-1	Veyo	37° 21' 28.5"	113° 40' 4.0"	Hayden (in prep.)
3-562	Cave Canyon	38° 18' 41.8"	112° 55' 40.4"	Rowley and others (2005)
3-528	Pine Park	37° 31' 40.9"	114° 01' 48.2"	Rowley and others (in prep.)
JP-3	Hilgard Mountain	38° 38' 23.0"	111° 31' 15.5"	Doelling (2004)
PR-28	Skinner Peaks	39° 23' 10"	111° 54' 00"	Felger and others (in prep.)
TS102103-5	Tickville Spring	40° 25' 05.7"	112° 03' 57.6"	Biek and others (2005)
TS33104-7	Tickville Spring	40° 25' 03.0"	112° 03' 59.8"	Biek and others (2005)
PR-29	Fountain Green North	39° 44' 28"	111° 42' 45"	Clark (in prep.)
PR-16	Skinner Peaks	39° 24' 33"	111° 53' 57"	Felger and others (in prep.)
TS33104-4	Tickville Spring	40° 29' 44.1"	112° 05' 05.7"	Biek and others (2005)
TS32904-3	Tickville Spring	40° 28' 26.5"	112° 04' 00.2"	Biek and others (2005)

Disclaimer

This Open-File release is intended as a data repository for technical analytical information gathered in support of various geologic mapping projects. The data are presented as received from the New Mexico Geochronology Research Laboratory and do not necessarily conform to UGS technical or editorial standards. Therefore, it may be premature for an individual or group to take actions based on the contents of this report.

Although this product represents the work of professional scientists, the Utah Department of Natural Resources, Utah Geological Survey, makes no warranty, expressed or implied, regarding its suitability for a particular use. The Utah Department of Natural Resources, Utah Geological Survey, shall not be liable under any circumstances for any direct, indirect, special, incidental, or consequential damages with respect to claims by users of this product.

References to geologic reports that cite or explain samples analyzed in this report

Biek, R.F., Solomon, B.J., Keith, J.D., and Smith, T.W., 2005, Geologic map of the Tickville Spring quadrangle, Salt Lake and Utah Counties, Utah: Utah Geological Survey Map 214, 2 plates, scale 1:24,000.

Clark, D.L., in preparation, Volcanic and intrusive rocks of central Utah: Utah Geological Survey Special Study.

Doelling, H.H., 2004, Interim geologic map of the east half of the Salina 30'x60' quadrangle, Emery, Sevier, and Wayne Counties, Utah: Utah Geological Survey Open-File Report 438, scale 1:62,500.

Felger, T.J., Clark, D.L., and Hylland, M.D., in preparation, Geologic map of the Skinner Peaks quadrangle, Juab and Sanpete Counties, Utah: Utah Geological Survey Map, scale 1:24,000.

Hayden, J.M., in preparation, Geologic map of the Veyo quadrangle, Washington County, Utah: Utah Geological Survey Map, scale 1:24,000.

Rowley, P.D., Vice, G.S., McDonald, R.E., Anderson, J.J., Machette, M.N., Maxwell, D.J., Ekren, E.B., Cunningham, C.G., Steven, T.A., and Wardlaw, B.R., 2005, Interim geologic map of the Beaver 30'x60' quadrangle, Beaver, Piute, Iron, and Garfield Counties, Utah: Utah Geological Survey Open-File Report 454, scale 1:100,000.

Rowley, P.D., Williams, V.S., Vice, G.S., Maxwell, D.J., Hacker, D.B., Snee, L.W., and Mackin, J.H., in preparation, Interim geologic map of the Cedar City 30'x60' quadrangle, Iron and Washington Counties, Utah: Utah Geological Survey Open-File Report, scale 1:100,000.

$^{40}Ar/^{39}Ar$ Geochronology Results

By

Lisa Peters

August 11, 2005

Prepared for

Robert Biek
Utah Geological Survey
1594 West North Temple, Suite 3110
PO Box 146100
Salt Lake City, Utah 84114-6100

New Mexico
Geochronology Research Laboratory
(NMGRL)

Co-Directors

Dr. Matthew T. Heizler

Dr. William C. McIntosh

Laboratory Technicians

Lisa Peters

Richard P. Esser

Internal Report #: NMGRL-IR-460

Introduction

Thirteen samples from various locations in Utah were submitted for dating by Bob Biek of the Utah Geological Survey. The rocks were varied in composition so a variety of mineral phases were separated. Sample TS9803-1, a rhyolite flow, did not contain what was felt to be datable mineral phases. This report presents results from the rest of the samples. This information is briefly summarized in Table 1.

Table 1. Brief summary of results.

Sample	Phase	Unit	Age±2σ (Ma)	Comments
VY9503-1	Groundmass concentrate	Magatsu Creek basaltic flow	0.68±0.33	isochron, low confidence
VY9303-1	Groundmass concentrate	Veyo basaltic flow	0.08±0.06	isochron, low confidence
3-562	Orthoclase	Mineral Mountains pluton	No age assigned	
3-528	Sanidine	Tuff of white rocks	16.27±0.17	
JP-3	Groundmass concentrate	Marysville volcanic field	25.86±0.19	
PR-28	Single crystal biotite	Painted Rocks tuff	29.81±0.14	
TS102103-5	Biotite	Traverse Mountain dacite dike	32.05±0.13	
TS33104-7	Groundmass concentrate	Traverse Mountain basaltic andesite	32.86±0.48	low confidence
PR-29	Biotite	Salt Creek andesite dike	34.72±0.08	isochron age
PR-16	Sanidine	Unit II tuff (Fernow tuff?)	35.19±0.14	
TS33104-4	Sanidine	Shaggy Peak Rhyolite Intrusion	35.49±0.13	
TS32904-3	Biotite	Step Mountain dike	36.26±0.18	

$^{40}Ar/^{39}Ar$ Analytical Methods and Results

Samples being prepared as groundmass concentrates were crushed and cleaned with dilute hydrochloric acid. Those being prepared as sanidine separates were crushed and cleaned with dilute hydrofluoric acid, while those being prepared as biotite separates were crushed and cleaned with only water. The analyzed phases were then separated with standard heavy liquid, magnetic separator and handpicking techniques. The mineral separates were loaded into aluminum discs and irradiated for 7 hours at the Nuclear Science Center in College Station, Texas.

The groundmass concentrates and biotite from PR-29 and TS32904-3 were analyzed with the furnace incremental heating age spectrum method. The sanidine was analyzed by the single-crystal laser fusion method. Biotite from PR-28 was step-heated (two steps) as single crystals with a CO_2 laser. The first steps were designed primarily to drive off atmospheric argon and thus increase the radiogenic yields and precision of the second steps. The age data for the more radiogenic, more precise steps from the biotite analyses and the sanidine total fusion data are displayed on a probability distribution diagram (Deino and Potts, 1992). Abbreviated analytical methods for the dated samples are given in Table 2, and details of the overall operation of the New Mexico Geochronology Research Laboratory are provided in the Appendix. The argon isotopic results are summarized in Tables 1 and 2 and listed in Tables 3-6.

Sanidine from samples 3-528 and TS33104-4 yield near Gaussian populations. Fifteen analyzed crystals of 3-528 were used to calculate a weighted mean age of 16.27±0.17 Ma with a MSWD value of 1.1(Figure 1, Table 3). MSWD values over one indicate scatter in the data not attributable to analytical error alone. The K/Ca values range from 12.8-25.8 and the radiogenic yields are consistently high and range from 81.7-97.3%. Thirteen of the analyzed TS33104-4 sanidine crystals were used to calculate a weighted mean age of 35.49±0.13 Ma with a MSWD value of 2.6 (Figure 2, Table 3). Three slightly older crystals were eliminated from the data set. The radiogenic yields of

the TS33140-4 sanidine were 96.3% and greater and the K/Ca values range from 59.4 to 167.8.

The spread in apparent ages for the sanidine from PR-16 is ~2-3 times greater than that for the previous two samples (Figure 3, Table 3). A weighted mean age of 35.19±0.14 Ma is calculated from all fifteen of the analyzed crystals. The MSWD value for this age is 11.3. The radiogenic yields are consistently high (94.9-99.7%) and the K/Ca values range in value from 60.5-218.4.

The A steps for PR-28 biotite had lower radiogenic yields (18-38% radiogenic vs. 60-89% radiogenic) and were less precise (an order of magnitude different) than the B steps (Tables 4 and 5). The B steps are shown plotted on Figure 4. All but the smallest, least precise analysis was used to calculate a weighted mean age of 29.81±0.14 Ma (MSWD = 1.0) for PR-28.

Biotite from PR-29 yielded a well-behaved age spectrum (Figure 5a, Table 6). The initial ~6% of the ^{39}Ar released yields relatively old apparent ages and low radiogenic yields. A weighted mean age of 34.78±0.13 Ma is calculated from the following 92.8% of the ^{39}Ar released. The radiogenic yields rise fairly consistently over this portion while the K/Ca values are somewhat oscillatory. The final ~4% of the ^{39}Ar released yields low apparent ages, radiogenic yields and K/Ca values. Steps A-K were evaluated with the inverse isochron technique were found to yield a ^{40}Ar/^{36}Ar intercept slightly over the atmospheric ratio of 295.5 (299.0±1.6, Figure 5b). The isochron age for these steps is 34.72±0.08 Ma (MSWD = 1.4).

Biotite from TS32904-3 also yielded a well-behaved age spectrum (Figure 6a). The initial ~8% of the ^{39}Ar released is disturbed. The K/Ca values and radiogenic yields over this portion of the spectrum are increasing. The following 91% of the ^{39}Ar was used to calculate a weighted mean age of 36.26±0.18 Ma (MSWD value of 3.2). The radiogenic yields climb over this portion of the spectrum while the K/Ca values rise and then fall. The last 1% of the spectrum yields decreasing apparent ages, K/Ca values and radiogenic yields. Inverse isochron analysis of steps A-J yield an isochron age of 36.24±0.14 Ma with a ^{40}Ar/^{36}Ar intercept of 295.9±4.2, well within error of the atmospheric intercept (Figure 6b).

JP-3 groundmass concentrate yields a fairly well-behaved age spectrum (Figure 7a). Apparent ages decrease over the initial 33% of the age spectrum. Radiogenic yields and K/Ca values increase over this portion of the spectrum. A weighted mean age of 25.86±0.19 Ma (MSWD value of 3.69) is calculated from the following 66.7% of the ^{39}Ar released. Radiogenic yields decrease consistently over this portion of the age spectrum while the K/Ca values increase slightly and then decrease. Steps A-I were evaluated with the inverse isochron technique and were found to have an atmospheric intercept (299.0±8.5) and an isochron age that agrees within error to the age spectrum age (26.01±0.62 Ma, Figure 7b).

TS102103-5 biotite yields a somewhat disturbed age spectrum (Figure 8a). Apparent ages increase over the initial 50% of the ^{39}Ar released. The apparent ages remain fairly constant over the remainder of the spectrum and a weighted mean of 32.05±0.13 Ma is calculated from this portion of the spectrum. The K/Ca values rise over the initial 23% of the spectrum and then fall throughout the remainder of the spectrum. Inverse isochron analysis of steps A-J reveal an atmospheric intercept (293.4±4.4) and an isochron age of 31.94±0.29 Ma (Figure 8b).

TS33104-7 groundmass concentrate yields a disturbed age spectrum (Figure 9a). Apparent ages show an overall decrease from the initial low temperature step to the fusion step (127-27.9 Ma). A weighted mean age of 32.86±0.48 Ma with a MSWD value of 5.94 is calculated from steps B-E. The K/Ca value and radiogenic yields show an increase over the initial 20-30% of the ^{39}Ar released. The K/Ca value decreases fairly consistently over the remainder of the spectrum while the radiogenic yields are oscillatory, increasing and then decreasing. Steps A-F were evaluated with the inverse isochron technique and revealed a $^{40}Ar/^{36}Ar$ intercept of 297±26 and an isochron age of 32.9±1.5 Ma (Figure 9b).

Groundmass concentrates from samples VY9503-1 and VY9303-1 yielded similar disturbed age spectra (Figures 10a and 11a). The spectra reveal old apparent ages in the early and late heating steps. The radiogenic yields are uniformly low (<10%) and the K/Ca values decrease fairly consistently over the entire age spectrum. Weighted mean ages are calculated over the relatively flat mid-portion of the spectra: 1.69±0.33,

VY9503-1 and 1.33±0.45 Ma, VY9303-1. Due to the uniformly low radiogenic yields, the data points cluster near the $^{36}Ar/^{40}Ar$ axis, when evaluated with the inverse isochron technique. The $^{40}Ar/^{36}Ar$ intercepts indicate slight excess Ar: VY9503-1, 304.7±2.6 and VY9303-1, 304.4±5.4 (Figures 10b and 11b). Accordingly, the isochron ages are younger (0.68±0.33 Ma, VY503-1; 0.08±0.06 Ma, VY9303-1) than the weighted mean ages calculated from the age spectra.

Orthoclase from 3-562 was analyzed as single crystals. The apparent ages of the fifteen analyzed crystals range from 12.20±0.07 Ma to 14.21±0.07 Ma (Figure 12). A weighted mean age calculated from these fifteen crystals would have a MSWD value of 77. The radiogenic yields (55.7-76.7%) are lower than expected (~90%) for a K-feldspar of this age.

Discussion

The weighted mean ages assigned to samples 3-528, TS33104-4, PR-16, PR-28, PR-29, TS32904-3 and JP-3 provide precise, reliable ages for the eruption or intrusion of these rocks. The increasing apparent ages and radiogenic yields revealed in the initial 50% of TS102103-5 age spectrum are suggestive of alteration and accompanying Ar loss. The integrated age of 32.11±0.53 Ma agrees within error to the weighted mean age calculated from the final 48.8% of the ^{39}Ar released from TS102103-5 biotite (32.05±0.13 Ma). This implies that the amount of Ar loss has been minimal so we have assigned 32.05±0.13 Ma as the age of intrusion for the Traverse Mountain dacite dike from which TS102103-5 was sampled. The decreasing apparent ages revealed by the TS33104-7 age spectrum suggests that there may have been ^{39}Ar recoil out of the high potassium sites and into the low potassium sites during irradiation. Recoil has the affect of increasing the ages of the parts of the spectrum controlled by mineral phases that have lost ^{39}Ar and decreasing the apparent ages of the parts of the spectrum controlled by those phases that have gained ^{39}Ar (Figure 13). In situations where recoil is suspected, the integrated age is usually assigned as the best estimate of the age of the sample. In this case, however, the A step is ~4 times the age of the other steps (127Ma) and it is unlikely this anomalously

old apparent age is caused solely by recoil. Excess Ar or analytical problems may also have contributed to the anomalously old age. If this is the case, the integrated age would not represent an accurate estimate of the sample's age. We have assigned the weighted mean age assigned to steps B-E (32.86±0.48 Ma) as our best estimate of this samples age. We caution that our confidence in number is not high. Saddle-shaped spectra such as those obtained for groundmass concentrates VY503-1 and VY9303-1 have been shown to be the result of excess Ar (Harrison and McDougall, 1981). Although the data points on the inverse isochron plots are highly clustered, the $^{40}Ar/^{36}Ar$ intercepts (VY9503-1, 304.7±2.6 and VY9303-1, 304.4±5.4) determined for these samples are indicative of excess Ar and we have chosen the isochron ages (VY9503-1, 0.68±0.33 Ma and VY9303-1, 0.08±0.06 Ma) as our best estimate of the age of these samples. Plutonic K-feldspar can have Ar closure temperatures as low as 150°C (McDougall and Harrison, 1999). If the Mineral Mountains pluton underwent slow cooling, the ages of the analyzed crystals of 3-562 would yield much younger ages than coexisting biotite (closure temperature of 300-350°C) or hornblende (closure temperature of 500-550°C) and yield more information about the cooling history of the pluton than the actual age of intrusion. The low radiogenic yields (55.7-76.7%) of the feldspar crystals suggest the Minerals Mountain pluton has undergone alteration. This is supported by the observation that the biotite separated from this rock is partially altered to chlorite. Given the concerns described above, we have not assigned an age to 3-562.

References Cited

Deino, A., and Potts, R., 1990. Single-Crystal $^{40}Ar/^{39}Ar$ dating of the Olorgesailie Formation, Southern Kenya Rift, J. Geophys. Res., 95, 8453-8470.

Deino, A., and Potts, R., 1992. Age-probability spectra from examination of single-crystal $^{40}Ar/^{39}Ar$ dating results: Examples from Olorgesailie, Southern Kenya Rift, Quat. International, 13/14, 47-53.

Harrison, T.M., and McDougall, I. 1981. Excess ^{40}Ar in metamorphic rocks from Broken Hill, New South Wales: Implications for $^{40}Ar/^{39}Ar$ age spectra and the thermal history of the region. Earth Planet. Sci. Lett., 55, 123-149.

Mahon, K.I., 1996. The New "York" regression: Application of an improved statistical method to geochemistry, International Geology Review, 38, 293-303.

Renne, P.R., Owens, T.L., DePaolo, D.J., Swisher, C.C., Deino, A.L., and Darner, D.B., 1998. Intercalibration of standards, absolute ages and uncertainties in $^{40}Ar.39AR$ dating, 145, 117-152.

Samson, S.D., and, Alexander, E.C., Jr., 1987. Calibration of the interlaboratory $^{40}Ar/^{39}Ar$ dating standard, Mmhb-1, Chem. Geol., 66, 27-34.

Steiger, R.H., and Jäger, E., 1977. Subcommission on geochronology: Convention on the use of decay constants in geo- and cosmochronology. Earth and Planet. Sci. Lett., 36, 359-362.

Taylor, J.R., 1982. An Introduction to Error Analysis: The Study of Uncertainties in Physical Measurements,. Univ. Sci. Books, Mill Valley, Calif., 270 p.

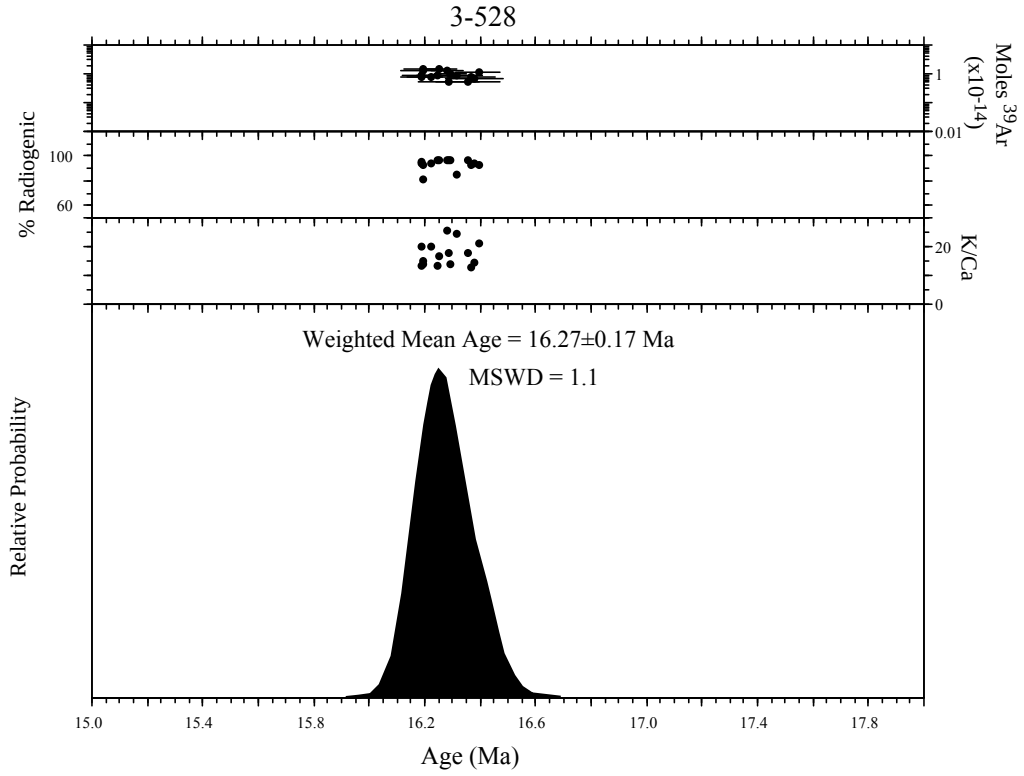

Figure 1. Age probability distribution diagram of 3-528 sanidine. All errors quoted at 2 sigma.

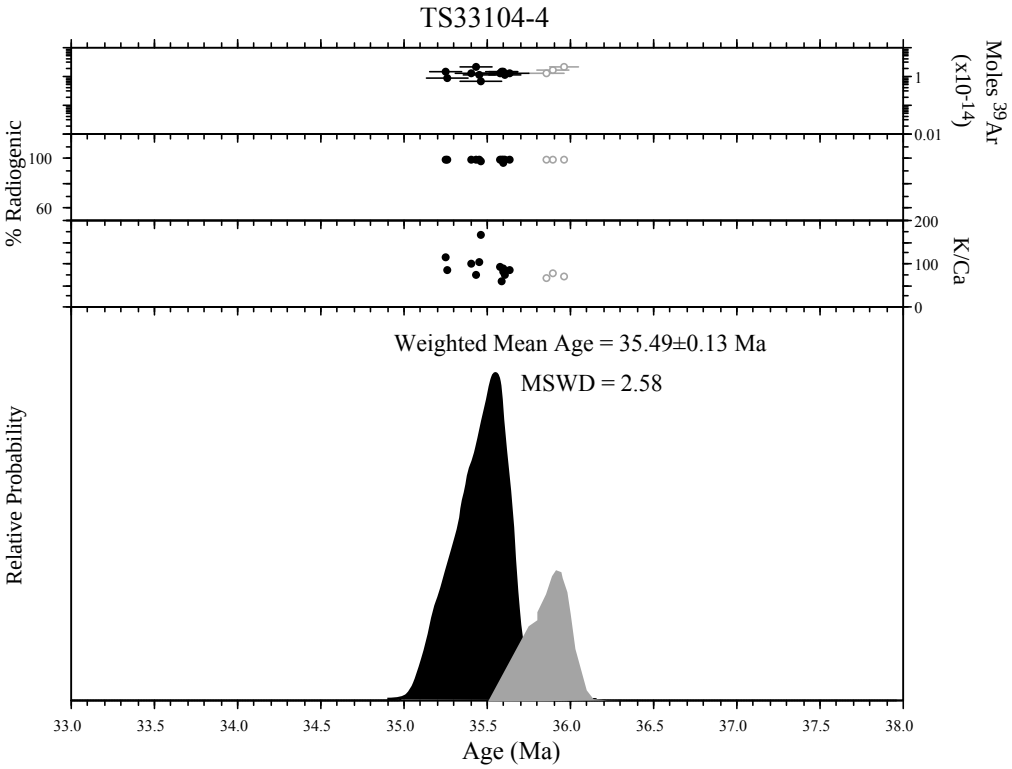

Figure 2 . Age probability distribution diagram of TS33104-4 sanidine. All errors quoted at 2 sigma.

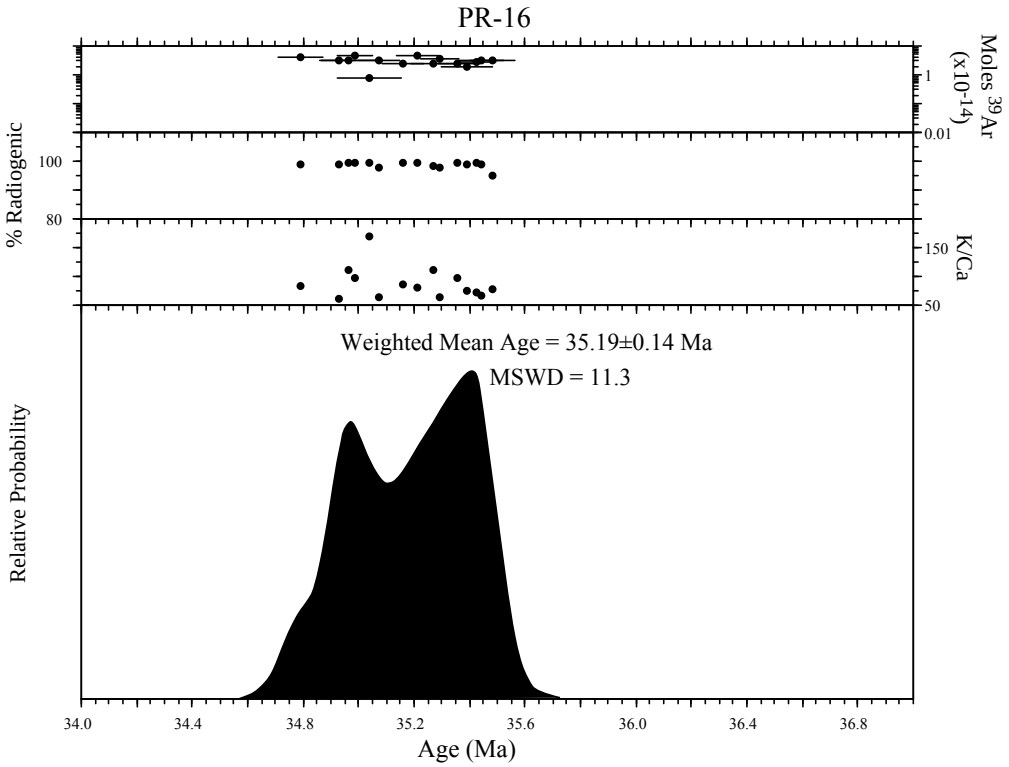

Figure 3. Age probability distribution diagram of PR-16 sanidine. All errors quoted at 2 sigma.

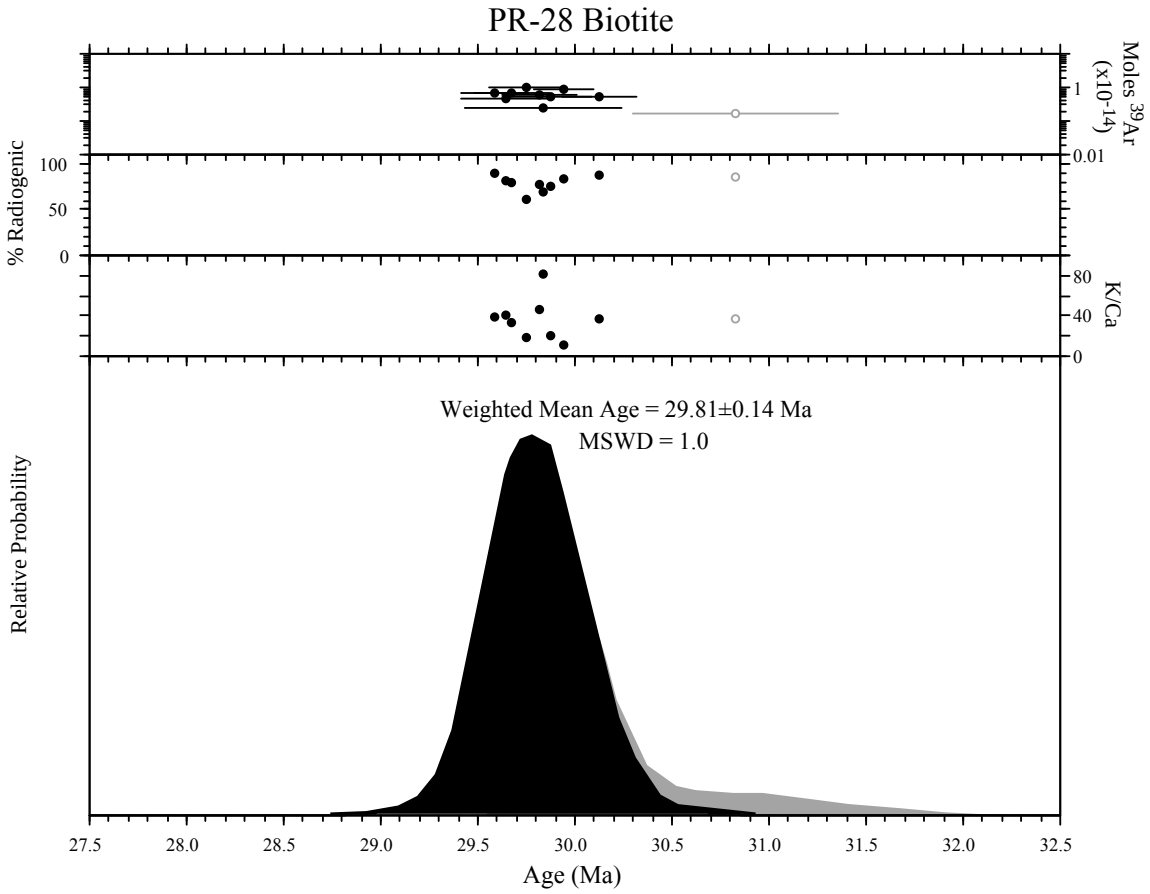

Figure 4 . Age probability distribution diagram of PR-28 single crystal biotite B-step analyses. All errors quoted at 2 sigma.

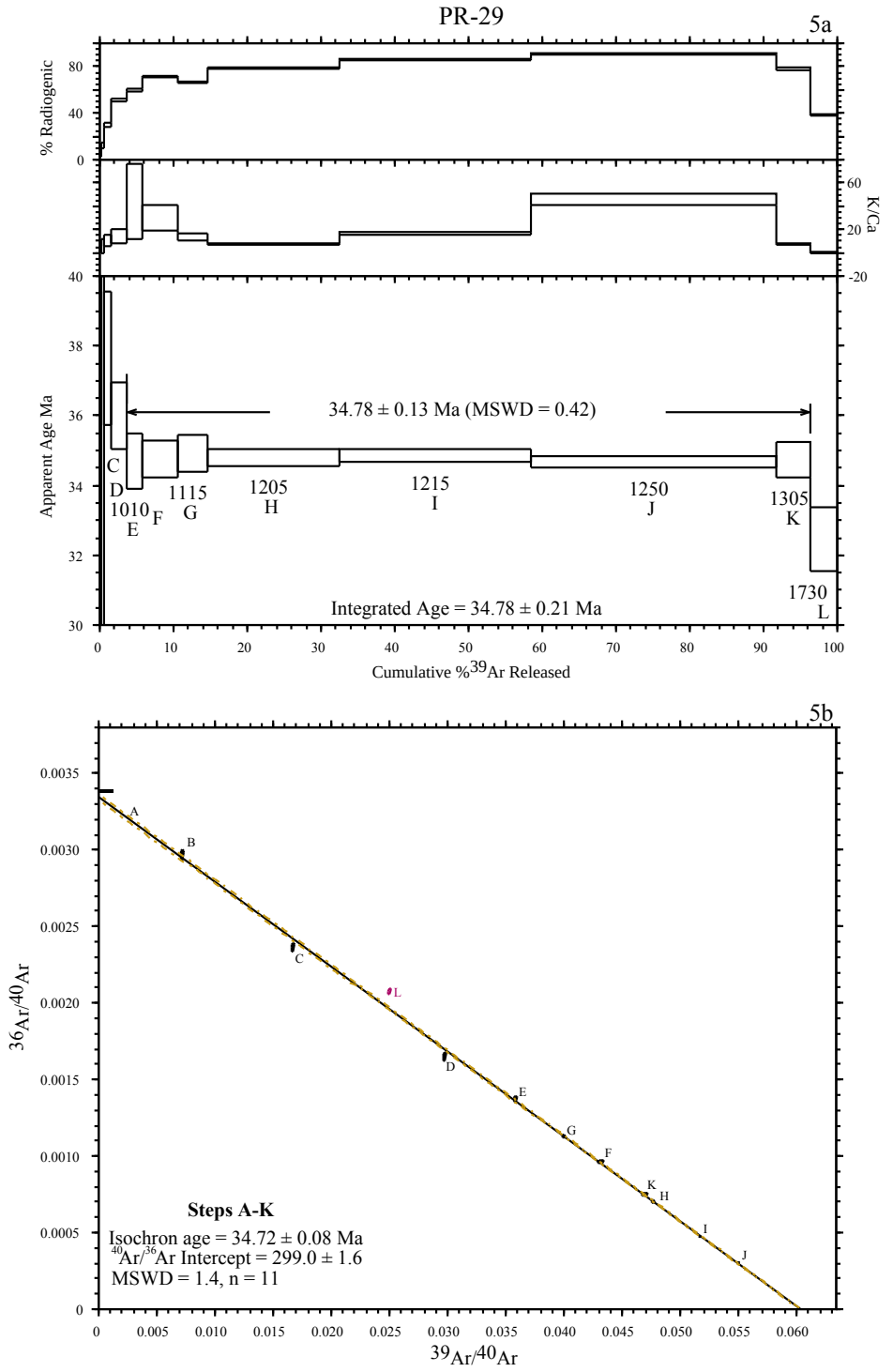

Figure 5. Age spectrum (5a) and isochron (5b) for PR-29 biotite. Point shown in purple not included in isochron age. All errors quoted at 2 sigma.

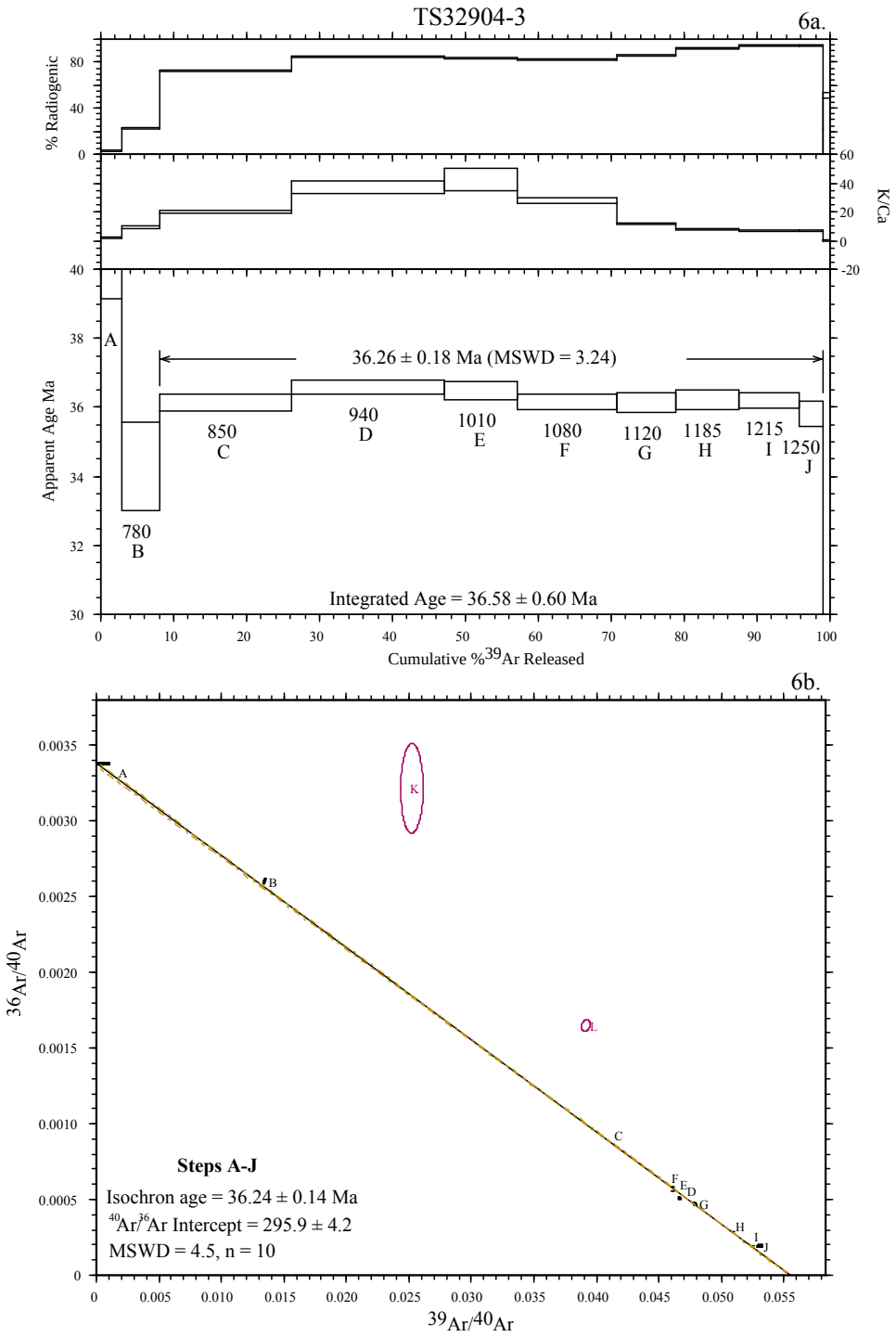

Figure 6. Age spectrum (6a) and isochron (6b) for TS32904-3 biotite. Points shown in purple not included in isochron. All errors quoted at 2 sigma.

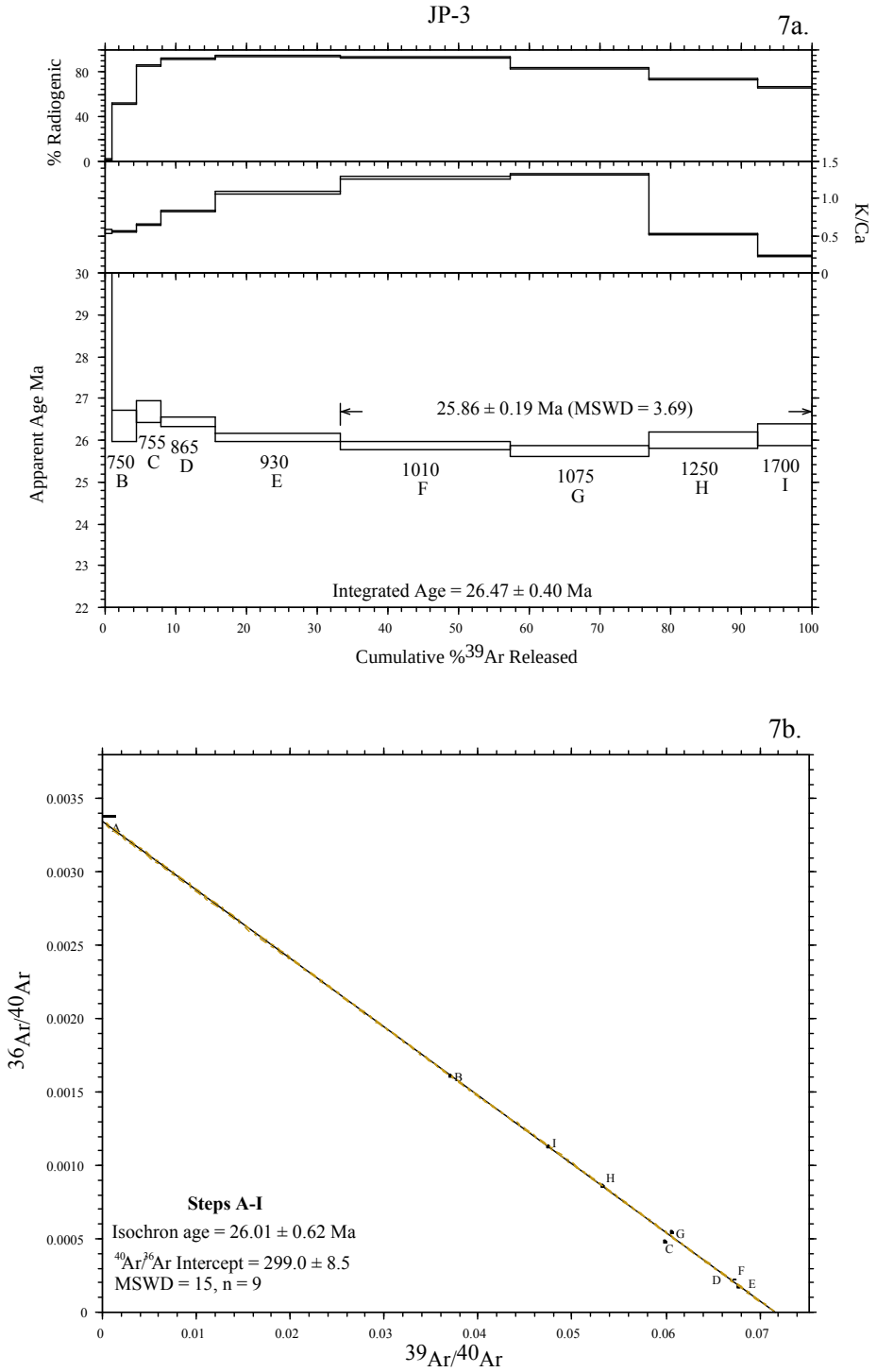

Figure 7. Age spectrum (1a) and isochron (b) for JP-3 groundmass concentrate. All errors quoted at 2 sigma.

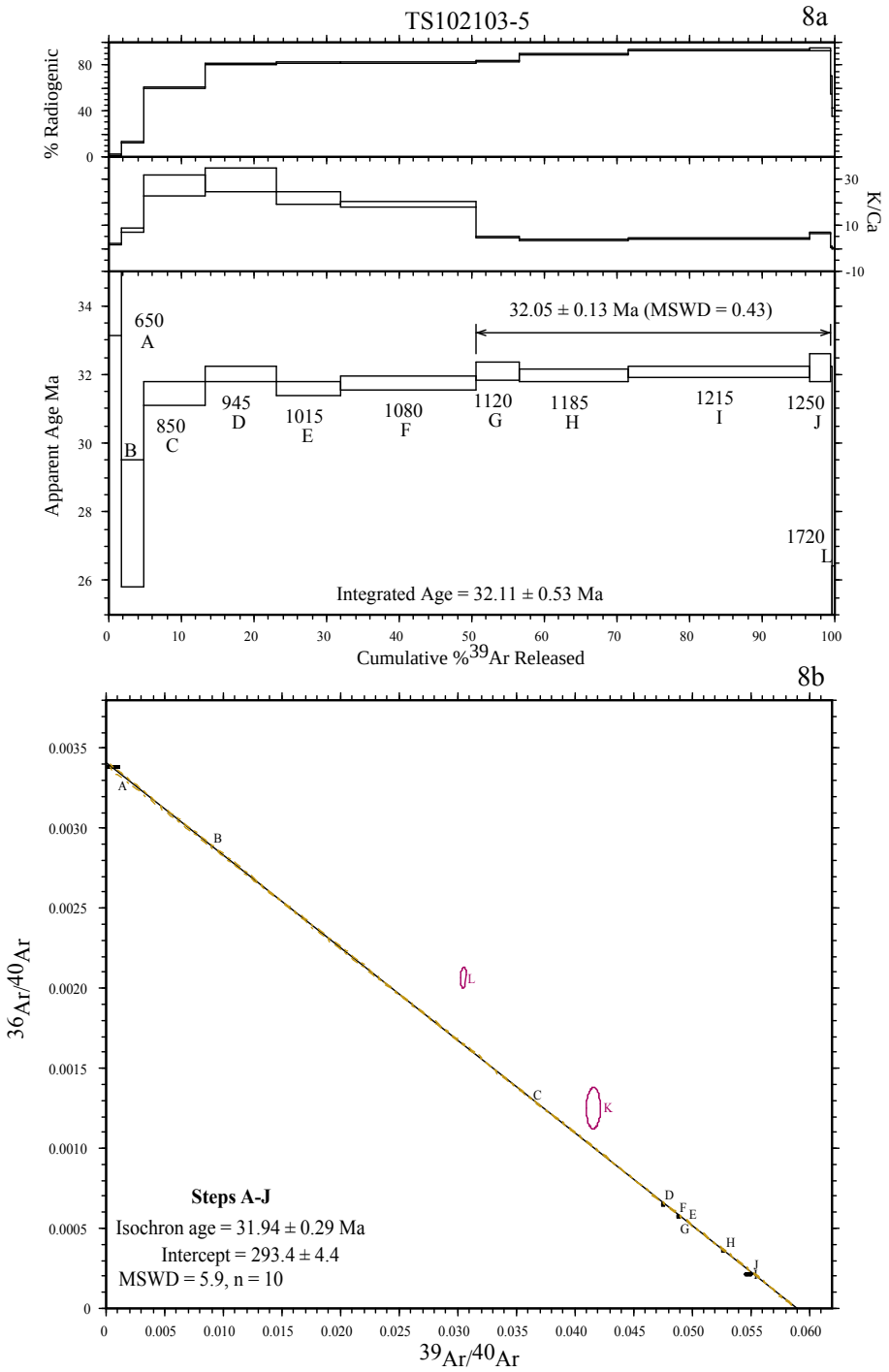

Figure 8. Age spectrum (8a) and isochron (8b) for TS102103-5 biotite. Points shown in purple not included on isochron. All errors quoted at 2 sigma.

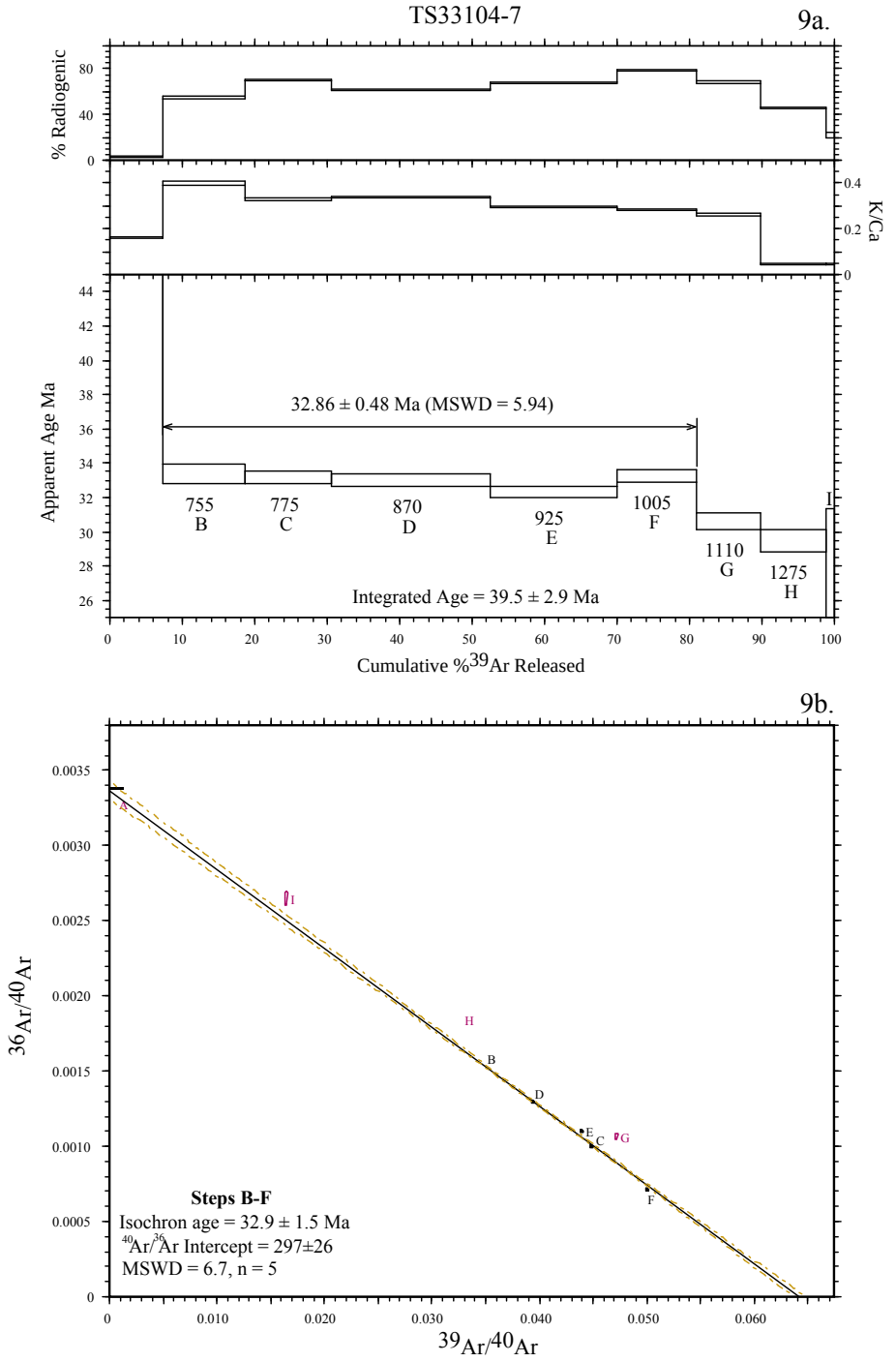

Figure 9. Age spectrum (9a) and isochron (9b) for TS33104-7 groundmass concentrate. Points shown in purple not included in isochron. All errors quoted at 2 sigma.

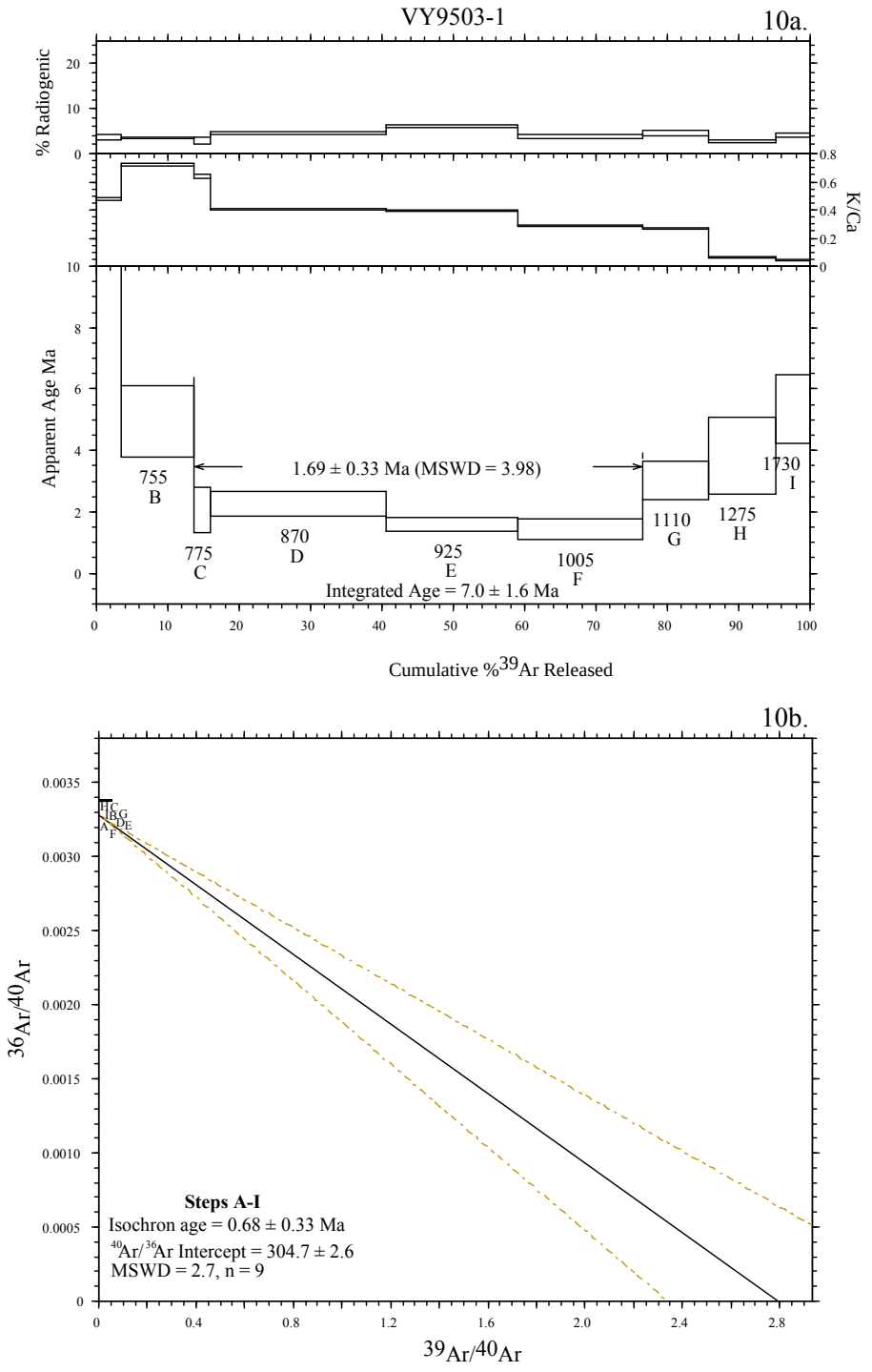

Figure 10. Age spectrum (10a) and isochron (10b) for VY9503-1 groundmass concentrate. All errors quoted at 2 sigma

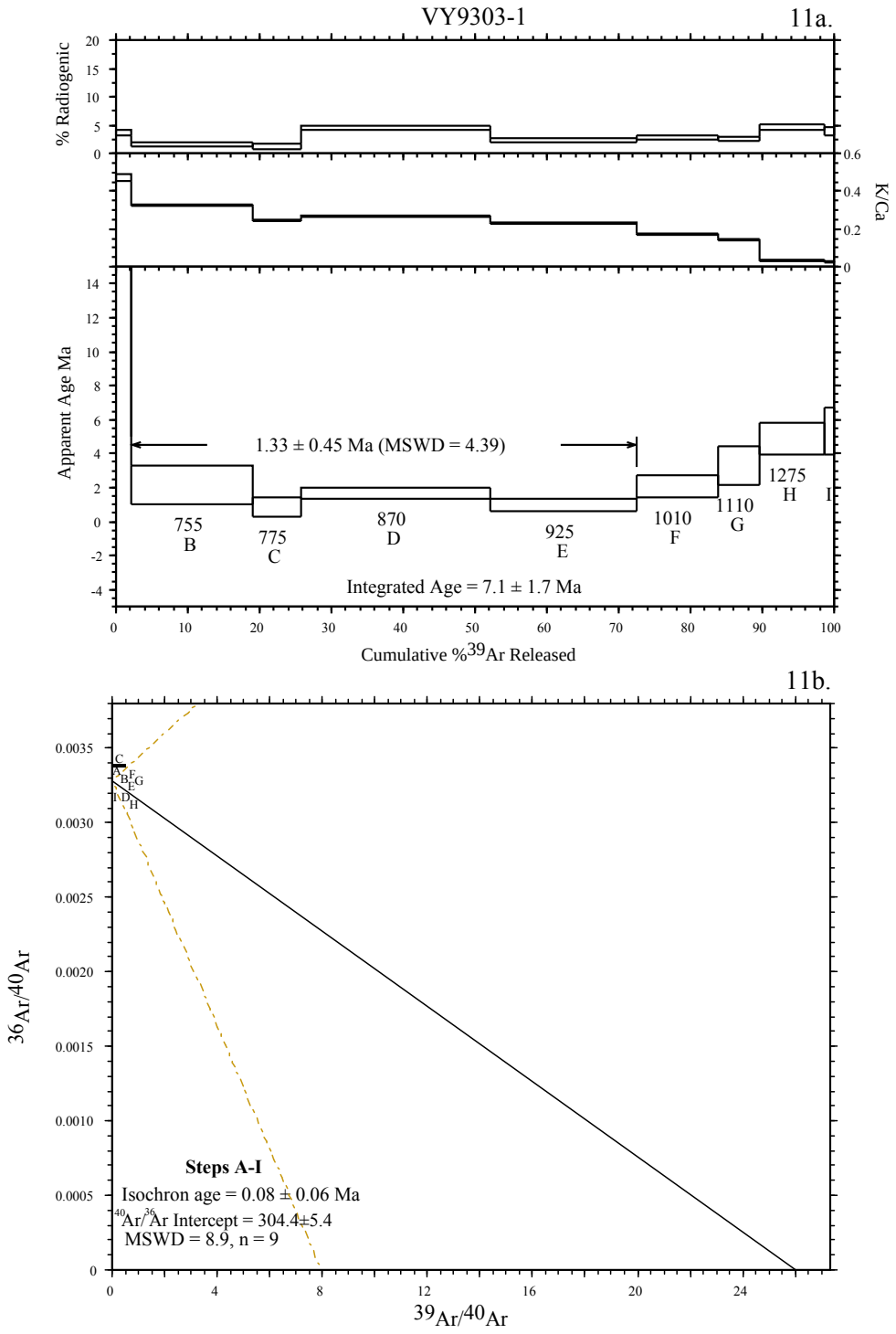

Figure 11. Age spectrum (1a) and isochron (b) for VY9303-1 groundmass concentrate. All errors quoted at 2 sigma.

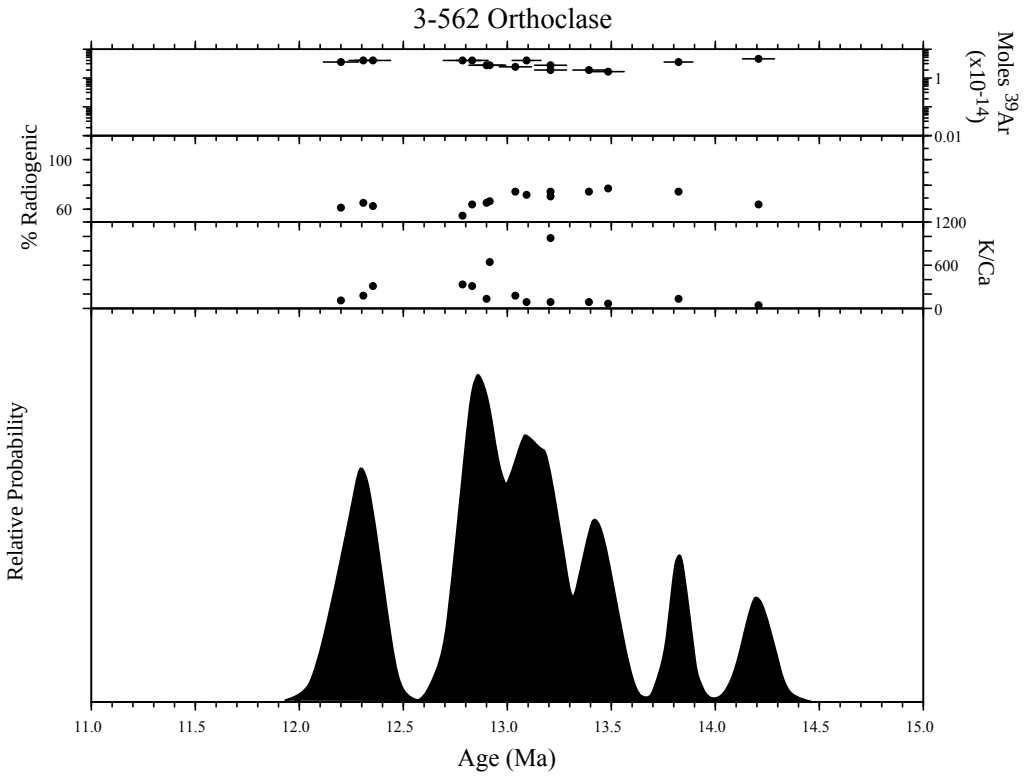

Figure 12 . Age probability distribution diagram of 3-562 orthoclase.

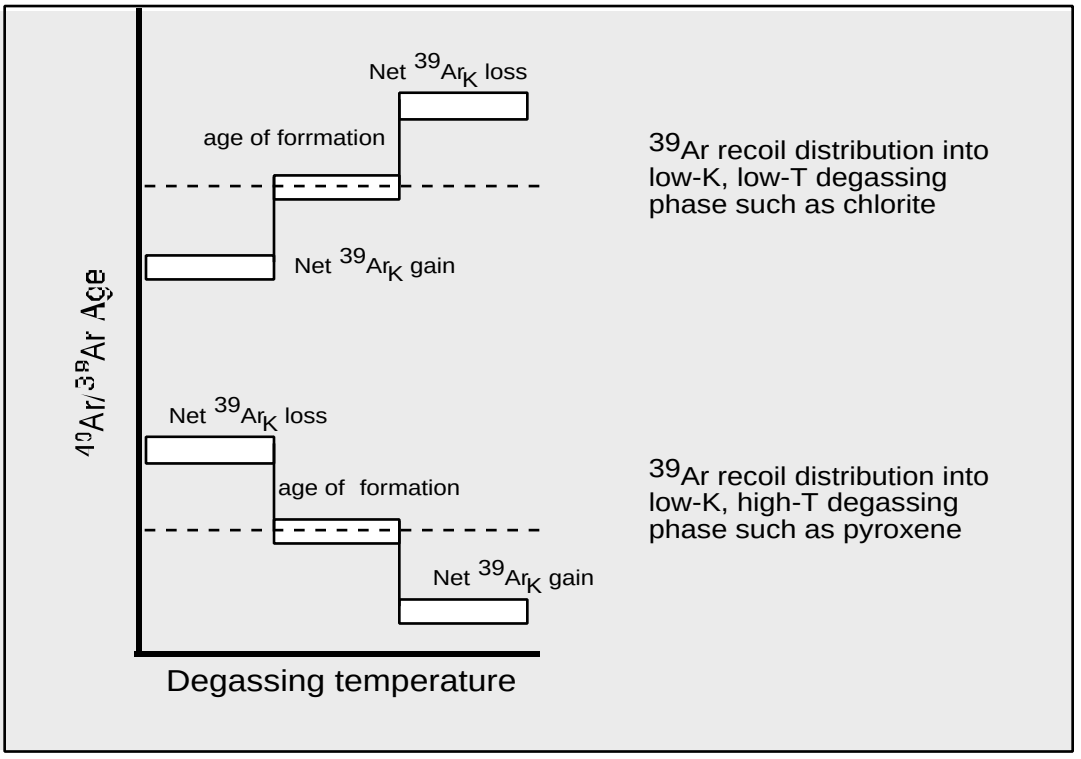

Figure 13. Cartoon showing potential effects of ^{39}Ar recoil on an otherwise flat age spectrum.

Table 2. Summary of $^{40}Ar/^{39}Ar$ results and analytical methods

Sample	Lab #	Irradiation	mineral	age analysis	# of crystals/steps	Age	±2σ	MSWD	40Ar/36Ar intercept	comments
VY9503-1	55176	NM-182	groundmass concentrate	furnace step-heat	9	0.68	0.33	12.7	304.7±2.6	isochron
VY9303-1	55173	NM-182	groundmass concentrate	furnace step-heat	9	0.08	0.06	4.39	304.4±5.4	isochron
3-562	55205	NM-182	orthoclase	single crystal total fusion	-	-	-	-	-	no age assigned
3-528	55204	NM-182	sanidine	single crystal total fusion	15	16.27	0.17	1.13	-	
JP-3	55183	NM-182	groundmass concentrate	furnace step-heat	3	25.86	0.19	3.69	-	
PR-28	55170	NM-182	biotite	single crystal step-heat	9	29.81	0.14		-	
TS102103-5	55171	NM-182	biotite	furnace step-heat	4	32.05	0.13	0.43	-	
TS33104-7	55174	NM-182	groundmass concentrate	furnace step-heat	4	32.86	0.48	0.34		
PR-29	55166	NM-182	biotite	furnace step-heat	11	34.72	0.08	1.4	299.0±1.6	isochron
PR-16	55163	NM-182	sanidine	single crystal total fusion	15	35.19	0.14	11.3	-	
TS33104-4	55162	NM-182	sanidine	single crystal total fusion	12	35.49	0.13	2.58	-	
TS32904-3	55167	NM-182	biotite	furnace step-heat	8	36.26	1.18	3.24	-	

Sample preparation and irradiation:
Minerals separated with standard heavy liquid, Franz Magnetic and hand-picking techniques.
Samples were loaded into a machined Al disc and irradiated for 10 hours in D-3 position, Nuclear Science Center, College Station, TX.
Neutron flux monitor Fish Canyon Tuff sanidine (FC-1). Assigned age = 28.02 Ma (Reine et al, 1998)
relative to Mmhb-1 at 520.4 Ma (Samson and Alexander, 1987).

Instrumentation:
Mass Analyzer Products 215-50 mass spectrometer on line with automated all-metal extraction system.
The groundmass concentrates were step-heated for 9 minutes using a Mo double-vacuum resistance furnace.
Reactive gases removed during furnace analysis by reaction with 3 SAES GP-50 getters, 2 operated at ~450°C and
1 at 20°C. Gas also exposed to a W filiment operated at ~2000°C.
Single crystal biotite were step-heated by a 50 watt Synrad CO_2 laser. Single crystal sanidine were fused by a 50 watt Synrad CO2 laser.
Reactive gases removed during a 4 minute reaction with 2 SAES GP-50 getters, 1 operated at ~450°C and
1 at 20°C. Gas also exposed to a W filament operated at ~2000°C and a cold finger operated at -140°C.

Analytical parameters:
Electron multiplier sensitivity averaged 2.13 x 10^{-16} moles/pA for furance analyses and 1.19 x 10-16 moles/pA.
Total system blank and background averaged 7870, 265, 8.0, 5.9, 0.16 x 10^{-18} moles at masses 40, 39, 38, 37 and 36, respectively for the furnace analyses.
Total system blank and background averaged 392, 6.7, 1.6, 1.1, 3.4 x 10^{-18} moles at masses 40, 39, 38, 37 and 36, respectively for the sanidine analyses.
Total system blank and background averaged 2380, 8.6, 2.5, 2.9, 10.0 x 10^{-18} moles at masses 40, 39, 38, 37 and 36, respectively for the biotite single crystal analyses.
J-factors determined to a precision of ± 0.1% by CO_2 laser-fusion of 6 single crystals from each of 6 or 10 radial positions around the irradiation tray.
Correction factors for interfering nuclear reactions were determined using K-glass and CaF_2 and are as follows:
$(^{40}Ar/^{39}Ar)_K = 0.00020\pm0.0003$; $(^{36}Ar/^{37}Ar)_{Ca} = 0.00028\pm0.000005$; and $(^{39}Ar/^{37}Ar)_{Ca} = 0.0007\pm0.00002$.

Table 3. $^{40}Ar/^{39}Ar$ analytical data.

ID	$^{40}Ar/^{39}Ar$	$^{37}Ar/^{39}Ar$	$^{36}Ar/^{39}Ar$ (x 10^{-3})	$^{39}Ar_K$ (x 10^{-15} mol)	K/Ca	$^{40}Ar^*$ (%)	Age (Ma)	±1σ (Ma)
3-528, sanidine, J=0.001551, D=1.0063, NM-182N, Lab#=55204								
11	6.070	0.0258	0.8857	5.526	19.8	95.7	16.19	0.06
12	6.216	0.0390	1.384	6.030	13.1	93.5	16.19	0.06
01	7.117	0.0369	4.424	8.995	13.8	81.7	16.19	0.07
09	6.257	0.0338	1.507	9.962	15.1	92.9	16.20	0.05
15	6.198	0.0252	1.273	5.307	20.2	94.0	16.22	0.07
06	6.029	0.0389	0.6800	6.212	13.1	96.7	16.24	0.07
10	6.038	0.0305	0.6982	11.012	16.7	96.6	16.25	0.05
04	6.022	0.0198	0.6068	9.231	25.8	97.0	16.28	0.05
08	6.090	0.0360	0.8303	6.696	14.2	96.0	16.29	0.05
13	6.062	0.0289	0.7335	3.972	17.7	96.5	16.29	0.10
05	6.888	0.0210	3.494	6.079	24.3	85.0	16.31	0.08
07	6.036	0.0288	0.5652	3.562	17.7	97.3	16.36	0.10
03	6.311	0.0399	1.487	5.516	12.8	93.1	16.37	0.07
14	6.253	0.0354	1.272	4.583	14.4	94.0	16.38	0.09
02	6.345	0.0240	1.558	8.131	21.2	92.8	16.40	0.06
Mean age ± 2σ		n=15	MSWD=1.13		17.3 ±8.3		16.27	0.17
3-562, sanidine, J=0.001576, D=1.0063, NM-182N, Lab#=55205								
06	6.943	0.0049	8.933	24.420	103.6	62.0	12.20	0.07
09	6.592	0.0027	7.615	29.335	186.8	65.9	12.30	0.06
04	6.919	0.0016	8.662	27.263	317.9	63.0	12.35	0.07
12	8.104	0.0016	12.16	27.163	326.6	55.7	12.79	0.07
07	7.026	0.0017	8.457	30.171	302.1	64.4	12.83	0.06
05	7.006	0.0041	8.303	19.766	124.7	65.0	12.90	0.07
10	6.864	0.0008	7.808	19.033	641.5	66.4	12.91	0.07
08	6.209	0.0027	5.442	18.459	185.9	74.1	13.04	0.06
03	6.396	0.0060	6.007	29.517	84.8	72.3	13.09	0.05
13	6.649	0.0005	6.728	20.675	988.8	70.1	13.21	0.06
02	6.230	0.0065	5.313	12.964	78.9	74.8	13.21	0.07
14	6.365	0.0057	5.540	13.576	88.8	74.3	13.40	0.06
11	6.204	0.0085	4.895	11.250	60.4	76.7	13.48	0.07
15	6.559	0.0039	5.680	24.207	131.0	74.4	13.83	0.05
01	7.781	0.0102	9.364	34.435	49.9	64.5	14.21	0.07

ID	$^{40}Ar/^{39}Ar$	$^{37}Ar/^{39}Ar$	$^{36}Ar/^{39}Ar$ (x 10^{-3})	$^{39}Ar_K$ (x 10^{-15} mol)	K/Ca	$^{40}Ar^*$ (%)	Age (Ma)	±1σ (Ma)
TS33104-4, sanidine, J=0.0011003, D=1.0063, NM-182H, Lab#=55162								
11	18.00	0.0045	0.2210	9.820	113.2	99.6	35.25	0.08
06	18.09	0.0059	0.5007	6.039	86.9	99.2	35.26	0.10
07	18.11	0.0051	0.3315	8.605	100.3	99.5	35.40	0.08
02	18.11	0.0067	0.2815	15.328	75.6	99.5	35.43	0.08
03	18.11	0.0049	0.2557	8.427	105.2	99.6	35.45	0.08
12	18.31	0.0030	0.8976	4.660	167.8	98.6	35.46	0.11
13	18.18	0.0055	0.2927	9.302	93.5	99.5	35.57	0.09
05	18.23	0.0086	0.4157	9.924	59.4	99.3	35.58	0.08
10	18.81	0.0059	2.375	9.127	87.2	96.3	35.59	0.07
01	18.31	0.0061	0.6639	10.379	83.3	98.9	35.60	0.07
09	18.16	0.0070	0.1550	8.352	72.9	99.8	35.61	0.08
15	18.31	0.0060	0.6185	8.714	85.5	99.0	35.64	0.09
14	*18.38*	*0.0078*	*0.4628*	*9.094*	*65.4*	*99.3*	*35.86*	*0.09*
08	*18.35*	*0.0065*	*0.3157*	*11.505*	*78.8*	*99.5*	*35.89*	*0.08*
04	*18.38*	*0.0071*	*0.2626*	*15.015*	*72.1*	*99.6*	*35.96*	*0.06*
Mean age ± 2σ		n=12	MSWD=2.58		94.2 ±54.7		35.49	0.13
PR-16, sanidine, J=0.0011509, D=1.0063, NM-182H, Lab#=55163								
01	17.08	0.0061	0.5522	28.765	83.2	99.0	34.80	0.07
02	17.18	0.0084	0.6432	23.078	60.5	98.9	34.95	0.05
06	17.07	0.0052	0.2257	31.160	97.8	99.6	34.97	0.05
04	17.13	0.0049	0.4185	22.860	105.0	99.3	34.98	0.09
11	17.47	0.0081	1.416	21.843	62.7	97.6	35.06	0.06
14	17.14	0.0023	0.1629	5.550	218.4	99.7	35.14	0.08
05	17.18	0.0062	0.2539	16.966	82.0	99.6	35.18	0.06
13	17.21	0.0064	0.3055	30.985	80.3	99.5	35.20	0.06
10	17.47	0.0046	1.097	16.488	111.5	98.1	35.25	0.07
08	17.53	0.0079	1.273	27.128	64.2	97.9	35.27	0.06
12	17.28	0.0052	0.3235	17.828	97.6	99.4	35.34	0.06
07	17.31	0.0069	0.3072	20.989	74.2	99.5	35.40	0.05
09	17.40	0.0076	0.5863	22.583	66.7	99.0	35.42	0.07
03	17.39	0.0072	0.5413	14.031	70.6	99.1	35.42	0.08
15	18.20	0.0063	3.144	22.534	81.3	94.9	35.51	0.06
Mean age ± 2σ		n=15	MSWD=11.27		90.4 ±77.5		35.19	0.14

Notes:

Isotopic ratios corrected for blank, radioactive decay, and mass discrimination, not corrected for interfering reactions.

Ages calculated relative to FC-1 Fish Canyon Tuff sanidine interlaboratory standard at 28.02 Ma.

Errors quoted for individual analyses include analytical error only, without interfering reaction or J uncertainties.

Mean age is weighted mean age of Taylor (1982). Mean age error is weighted error of the mean (Taylor, 1982), multiplied by the root of the MSWD where MSWD>1, and also incorporates uncertainty in J factors and irradiation correction uncertainties.

Decay constants and isotopic abundances after Steiger and Jaeger (1977).

symbol preceding sample ID denotes analyses excluded from mean age calculations.

Discrimination = 1.0063 ± 0.001

Correction factors:

$(^{39}Ar/^{37}Ar)_{Ca}$ = 0.0007 ± 5e-05

$(^{36}Ar/^{37}Ar)_{Ca}$ = 0.00028 ± 1e-05

$(^{38}Ar/^{39}Ar)_{K}$ = 0.0133

$(^{40}Ar/^{39}Ar)_{K}$ = 0 ± 0.0004

Table 4. $^{40}Ar/^{39}Ar$ analytical data.

ID	$^{40}Ar/^{39}Ar$	$^{37}Ar/^{39}Ar$	$^{36}Ar/^{39}Ar$ (x 10^{-3})	$^{39}Ar_K$ (x 10^{-15} mol)	K/Ca	$^{40}Ar^*$ (%)	Age (Ma)	±1σ (Ma)
PR-28, biotite, J=0.0010279, D=1.0063, NM-182H, Lab#=55170								
08B	18.05	0.0131	6.657	6.907	39.1	89.1	29.59	0.15
10B	19.79	0.0123	12.42	4.528	41.6	81.5	29.64	0.21
05B	20.45	0.0150	14.61	6.678	34.1	78.9	29.68	0.17
06B	26.88	0.0266	36.23	9.713	19.1	60.2	29.75	0.17
02B	20.97	0.0110	16.10	6.230	46.3	77.3	29.81	0.18
03B	23.16	0.0063	23.47	2.406	81.1	70.1	29.84	0.39
04B	21.81	0.0257	18.86	5.581	19.9	74.5	29.87	0.20
09B	19.27	0.0444	10.13	8.497	11.5	84.5	29.95	0.13
07B	18.78	0.0135	8.115	5.568	37.9	87.2	30.13	0.17
01B	*19.79*	*0.0137*	*10.22*	*1.733*	*37.3*	*84.7*	*30.83*	*0.51*
Mean age ± 2σ	n=9	MSWD=1.04			36.7 ±40.8		29.81	0.14

Notes:

Isotopic ratios corrected for blank, radioactive decay, and mass discrimination, not corrected for interfering reactions.

Ages calculated relative to FC-1 Fish Canyon Tuff sanidine interlaboratory standard at 28.02 Ma.

Errors quoted for individual analyses include analytical error only, without interfering reaction or J uncertainties.

Mean age is weighted mean age of Taylor (1982). Mean age error is weighted error of the mean (Taylor, 1982), multiplied by the root of the MSWD where MSWD>1, and also incorporates uncertainty in J factors and irradiation correction uncertainties.

Decay constants and isotopic abundances after Steiger and Jaeger (1977).

symbol preceding sample ID denotes analyses excluded from mean age calculations.

Discrimination = 1.0063 ± 0.001

Correction factors:

$(^{39}Ar/^{37}Ar)_{Ca}$ = 0.0007 ± 5e-05

$(^{36}Ar/^{37}Ar)_{Ca}$ = 0.00028 ± 1e-05

$(^{38}Ar/^{39}Ar)_{K}$ = 0.0133

$(^{40}Ar/^{39}Ar)_{K}$ = 0 ± 0.0004

Table 5. $^{40}Ar/^{39}Ar$ analytical data.

ID	Power (Watts)	$^{40}Ar/^{39}Ar$	$^{37}Ar/^{39}Ar$	$^{36}Ar/^{39}Ar$ (x 10^{-3})	$^{39}Ar_K$ (x 10^{-15} mol)	K/Ca	$^{40}Ar^*$ (%)	^{39}Ar (%)	Age (Ma)	±1σ (Ma)
PR-28, bi, J=0.0010279±0.12%, D=1.0063±0.001, NM-182H, Lab#=55170-01										
A	2	55.66	0.3922	125.7	0.102	1.3	33.3	5.5	34.1	7.9
B	4	19.79	0.0137	10.22	1.73	37.3	84.7	100.0	30.83	0.51
Integrated age ± 2σ			n=2		1.83				31.0	1.3
Plateau ± 2σ	steps A-B		n=2	MSWD=0.17	1.83	35.3		100.0	30.8	1.0
PR-28, bi, J=0.0010279±0.12%, D=1.0063±0.001, NM-182H, Lab#=55170-02										
A	2	81.00	0.2172	229.8	0.177	2.3	16.2	2.8	24.2	4.9
B	4	20.97	0.0110	16.10	6.23	46.3	77.3	100.0	29.81	0.18
Integrated age ± 2σ			n=2		6.41				29.66	0.45
Plateau ± 2σ	steps A-B		n=2	MSWD=1.33	6.41	45.1		100.0	29.81	0.41
PR-28, bi, J=0.0010279±0.12%, D=1.0063±0.001, NM-182H, Lab#=55170-03										
A	2	45.43	0.1597	90.27	0.134	3.2	41.3	5.3	34.5	5.9
B	4	23.16	0.0063	23.47	2.41	81.1	70.1	100.0	29.84	0.39
Integrated age ± 2σ			n=2		2.54				30.08	0.97
Plateau ± 2σ	steps A-B		n=2	MSWD=0.61	2.54	77.0		100.0	29.86	0.78
PR-28, bi, J=0.0010279±0.12%, D=1.0063±0.001, NM-182H, Lab#=55170-04										
A	2	59.54	0.2513	147.5	0.278	2.0	26.8	4.7	29.4	3.1
B	4	21.81	0.0257	18.86	5.58	19.9	74.5	100.0	29.87	0.20
Integrated age ± 2σ			n=2		5.86				29.85	0.49
Plateau ± 2σ	steps A-B		n=2	MSWD=0.03	5.86	19.0		100.0	29.87	0.40
PR-28, bi, J=0.0010279±0.12%, D=1.0063±0.001, NM-182H, Lab#=55170-05										
A	2	94.47	0.2286	261.8	0.612	2.2	18.1	8.4	31.5	1.8
B	4	20.45	0.0150	14.61	6.68	34.1	78.9	100.0	29.68	0.17
Integrated age ± 2σ			n=2		7.29				29.83	0.47
Plateau ± 2σ	steps A-B		n=2	MSWD=0.98	7.29	31.4		100.0	29.69	0.35
PR-28, bi, J=0.0010279±0.12%, D=1.0063±0.001, NM-182H, Lab#=55170-06										
A	2	99.21	0.3524	273.7	0.273	1.4	18.5	2.7	33.8	3.5
B	4	26.88	0.0266	36.23	9.71	19.1	60.2	100.0	29.75	0.17
Integrated age ± 2σ			n=2		9.99				29.86	0.41
Plateau ± 2σ	steps A-B		n=2	MSWD=1.33	9.99	18.7		100.0	29.76	0.41
PR-28, bi, J=0.0010279±0.12%, D=1.0063±0.001, NM-182H, Lab#=55170-07										
A	2	52.38	0.0311	109.2	0.171	16.4	38.4	3.0	36.9	4.7
B	4	18.78	0.0135	8.115	5.57	37.9	87.2	100.0	30.13	0.17
Integrated age ± 2σ			n=2		5.74				30.33	0.44
Plateau ± 2σ	steps A-B		n=2	MSWD=2.09	5.74	37.2		100.0	30.14	0.49

ID	Power (Watts)	$^{40}Ar/^{39}Ar$	$^{37}Ar/^{39}Ar$	$^{36}Ar/^{39}Ar$ (x 10^{-3})	$^{39}Ar_K$ (x 10^{-15} mol)	K/Ca	$^{40}Ar^*$ (%)	^{39}Ar (%)	Age (Ma)	±1σ (Ma)
PR-28, bi, J=0.0010279±0.12%, D=1.0063±0.001, NM-182H, Lab#=55170-08										
A	2	60.09	0.3619	147.8	0.151	1.4	27.4	2.1	30.3	5.7
B	4	18.05	0.0131	6.657	6.91	39.1	89.1	100.0	29.59	0.15
Integrated age ± 2σ			n=2		7.06				29.61	0.39
Plateau ± 2σ	steps A-B		n=2	MSWD=0.01	7.06	38.3		100.0	29.59	0.31
PR-28, bi, J=0.0010279±0.12%, D=1.0063±0.001, NM-182H, Lab#=55170-09										
A	2	82.34	0.2431	212.6	0.232	2.1	23.7	2.7	35.9	3.9
B	4	19.27	0.0444	10.13	8.50	11.5	84.5	100.0	29.95	0.13
Integrated age ± 2σ			n=2		8.73				30.10	0.35
Plateau ± 2σ	steps A-B		n=2	MSWD=2.28	8.73	11.3		100.0	29.95	0.40
PR-28, bi, J=0.0010279±0.12%, D=1.0063±0.001, NM-182H, Lab#=55170-10										
A	2	112.9	0.4827	321.4	0.146	1.1	16.0	3.1	33.1	5.8
B	4	19.79	0.0123	12.42	4.53	41.6	81.5	100.0	29.64	0.21
Integrated age ± 2σ			n=2		4.67				29.75	0.56
Plateau ± 2σ	steps A-B		n=2	MSWD=0.36	4.67	40.4		100.0	29.65	0.42

Isotopic ratios corrected for blank, radioactive decay, and mass discrimination, not corrected for interfering reactions.
Ages calculated relative to FC-1 Fish Canyon Tuff sanidine interlaboratory standard at 28.02 Ma.
Errors quoted for individual analyses include analytical error only, without interfering reaction or J uncertainties.
Integrated age calculated by recombining isotopic measurements of all steps.
Integrated age error calculated by recombining errors of isotopic measurements of all steps.
Plateau age is inverse-variance-weighted mean of selected steps.
Plateau age error is inverse-variance-weighted mean error (Taylor, 1982) times root MSWD where MSWD>1.
Plateau and integrated ages incorporate uncertainties in interferring reaction corrections and J factors.
Decay constants and isotopic abundances after Steiger and Jaeger (1977).
# symbol preceding sample ID denotes analyses excluded from plateau age calculations.
Discrimination = 1.0063 ± 0.001
Correction factors:
$(^{39}Ar/^{37}Ar)_{Ca}$ = 0.0007 ± 5e-05
$(^{36}Ar/^{37}Ar)_{Ca}$ = 0.00028 ± 1e-05
$(^{38}Ar/^{39}Ar)_{K}$ = 0.0133
$(^{40}Ar/^{39}Ar)_{K}$ = 0 ± 0.0004

Table 6. $^{40}Ar/^{39}Ar$ analytical data.

ID	Power (°C)	$^{40}Ar/^{39}Ar$	$^{37}Ar/^{39}Ar$	$^{36}Ar/^{39}Ar$ (x 10^{-3})	$^{39}Ar_K$ (x 10^{-15} mol)	K/Ca	$^{40}Ar^*$ (%)	^{39}Ar (%)	Age (Ma)	±1σ (Ma)
PR-29, bi, J=0.0011731±0.11%, D=1.0063±0.001, NM-182H, Lab#=55166-01										
A	*650*	*430.5*	*0.2483*	*1404.0*	*0.319*	*2.1*	*3.6*	*0.2*	*32.68*	*6.85*
B	*750*	*139.2*	*0.0929*	*412.7*	*0.417*	*5.5*	*12.4*	*0.5*	*36.20*	*3.74*
C	*850*	*59.85*	*0.0491*	*141.7*	*1.46*	*10.4*	*30.0*	*1.6*	*37.63*	*0.96*
D	*920*	*33.55*	*0.0365*	*55.43*	*2.83*	*14.0*	*51.2*	*3.6*	*36.00*	*0.48*
E	1000	27.86	0.0115	38.26	3.04	44.2	59.4	5.8	34.69	0.39
F	1075	23.15	0.0172	22.22	6.49	29.6	71.6	10.5	34.76	0.26
G	1110	25.01	0.0372	28.24	5.66	13.7	66.6	14.6	34.93	0.26
H	1180	20.98	0.0661	14.84	24.9	7.7	79.1	32.5	34.81	0.12
I	1210	19.33	0.0306	9.125	36.0	16.7	86.1	58.5	34.87	0.09
J	1250	18.18	0.0111	5.520	46.0	45.8	91.0	91.7	34.69	0.08
K	1300	21.28	0.0679	15.99	6.53	7.5	77.8	96.4	34.73	0.25
L	*1720*	*39.96*	*1.675*	*83.38*	*4.98*	*0.30*	*38.7*	*100.0*	*32.46*	*0.46*
Integrated age ± 2σ			n=12		138.6				34.75	0.21
Plateau ± 2σ	steps E-K		n=7	MSWD=0.42	128.6	26.1		92.8	34.78	0.13
Isochron±2σ	steps A-I		n=9	MSWD = 1.4	$^{40}Ar/^{36}Ar$=299.0±1.6				34.72	0.08
TS32904-3, bi, J=0.001127±0.12%, D=1.0063±0.001, NM-182H, Lab#=55167-01										
A	*650*	*881.7*	*0.2030*	*2893.4*	*4.85*	*2.5*	*3.0*	*2.9*	*53.57*	*7.20*
B	*750*	*73.99*	*0.0545*	*192.8*	*8.63*	*9.4*	*23.0*	*8.1*	*34.29*	*0.63*
C	850	24.53	0.0257	22.26	30.0	19.9	73.2	26.1	36.13	0.12
D	920	21.41	0.0139	10.94	35.0	36.7	84.9	47.1	36.58	0.10
E	1000	21.67	0.0120	11.99	16.6	42.5	83.7	57.0	36.48	0.13
F	1075	21.68	0.0183	12.58	22.8	27.9	82.9	70.7	36.16	0.11
G	1110	20.89	0.0425	9.948	13.4	12.0	85.9	78.8	36.13	0.14
H	1180	19.65	0.0653	5.624	14.5	7.8	91.6	87.5	36.22	0.13
I	1210	19.05	0.0712	3.665	13.9	7.2	94.3	95.8	36.18	0.11
J	1250	18.85	0.0739	3.622	5.38	6.9	94.4	99.1	35.80	0.18
K	*1300*	*39.60*	*3.302*	*128.2*	*0.087*	*0.15*	*5.0*	*99.1*	*4.06*	*6.95*
L	*1720*	*25.47*	*3.744*	*43.05*	*1.44*	*0.14*	*51.3*	*100.0*	*26.42*	*0.63*
Integrated age ± 2σ			n=12		166.5				36.58	0.60
Plateau ± 2σ	steps C-J		n=8	MSWD=3.24	151.5	24.0		91.0	36.26	0.18
TS102103-5, bi, J=0.0010542±0.14%, D=1.0063±0.001, NM-182H, Lab#=55171-01										
A	*650*	*1347.1*	*0.2877*	*4461.0*	*2.78*	*1.8*	*2.1*	*1.7*	*54.09*	*10.49*
B	*750*	*113.1*	*0.0636*	*333.3*	*4.84*	*8.0*	*12.9*	*4.8*	*27.65*	*0.93*
C	*850*	*27.72*	*0.0184*	*37.39*	*13.6*	*27.7*	*60.2*	*13.3*	*31.44*	*0.17*
D	*920*	*21.02*	*0.0171*	*13.68*	*15.4*	*29.9*	*80.8*	*23.0*	*32.01*	*0.12*
E	*1000*	*20.34*	*0.0233*	*12.14*	*14.2*	*21.9*	*82.4*	*31.9*	*31.59*	*0.10*
F	*1075*	*20.49*	*0.0263*	*12.36*	*29.7*	*19.4*	*82.2*	*50.5*	*31.75*	*0.09*
G	1110	20.49	0.1017	11.77	9.62	5.0	83.1	56.6	32.09	0.13
H	1180	18.99	0.1358	6.909	23.8	3.8	89.3	71.6	31.98	0.09
I	1210	18.21	0.1173	4.082	39.6	4.4	93.4	96.5	32.07	0.07
J	1250	18.22	0.0760	3.899	4.63	6.7	93.7	99.4	32.19	0.20
K	*1300*	*24.01*	*0.5319*	*30.13*	*0.365*	*0.96*	*63.1*	*99.6*	*28.61*	*1.82*
L	*1720*	*32.70*	*3.821*	*68.76*	*0.605*	*0.13*	*38.8*	*100.0*	*24.04*	*1.19*
Integrated age ± 2σ			n=12		159.1				32.11	0.53
Plateau ± 2σ	steps G-J		n=4	MSWD=0.43	77.7	4.4		48.8	32.05	0.13

ID	Power (°C)	$^{40}Ar/^{39}Ar$	$^{37}Ar/^{39}Ar$	$^{36}Ar/^{39}Ar$ (x 10^{-3})	$^{39}Ar_K$ (x 10^{-15} mol)	K/Ca	$^{40}Ar^*$ (%)	^{39}Ar (%)	Age (Ma)	±1σ (Ma)
TS33104-7, Groundmass Concentrate, J=0.0011803±0.23%, D=1.0063±0.001, NM-182J, Lab#=55174-01										
A	*650*	*2052.8*	*3.141*	*6739.6*	*5.01*	*0.16*	*3.0*	*7.4*	*126.64*	*17.27*
B	725	28.80	1.279	44.32	7.68	0.40	54.9	18.7	33.38	0.29
C	775	22.26	1.563	22.62	7.97	0.33	70.5	30.5	33.17	0.18
D	825	25.33	1.510	33.22	14.8	0.34	61.7	52.4	33.03	0.18
E	900	22.69	1.709	25.49	11.9	0.30	67.4	70.1	32.33	0.16
F	*1000*	*19.95*	*1.792*	*14.75*	*7.33*	*0.28*	*78.9*	*80.9*	*33.25*	*0.19*
G	*1100*	*21.17*	*1.960*	*23.20*	*6.03*	*0.26*	*68.4*	*89.8*	*30.60*	*0.25*
H	*1275*	*30.43*	*10.32*	*58.99*	*6.13*	*0.049*	*45.5*	*98.8*	*29.47*	*0.34*
I	*1725*	*60.26*	*10.54*	*162.5*	*0.781*	*0.048*	*21.7*	*100.0*	*27.90*	*1.71*
Integrated age ± 2σ			n=9		67.7				39.5	2.9
Plateau ± 2σ	steps B-E		n=4	MSWD=5.94	42.4	0.34		62.7	32.86	0.48
VY9303-1, Groundmass Concentrate, J=0.0011682±0.16%, D=1.0063±0.001, NM-182J, Lab#=55173-01										
A	*650*	*3104.6*	*1.080*	*10112.1*	*8.17*	*0.47*	*3.8*	*2.1*	*230.48*	*26.33*
B	725	63.52	1.554	211.9	66.3	0.33	1.6	19.1	2.16	0.57
C	775	31.25	2.084	105.0	26.1	0.24	1.3	25.7	0.85	0.30
D	825	17.54	1.914	57.23	102.8	0.27	4.5	52.1	1.66	0.15
E	900	19.54	2.160	65.18	79.9	0.24	2.3	72.5	0.97	0.18
F	*1000*	*35.97*	*2.865*	*119.2*	*44.5*	*0.18*	*2.7*	*83.9*	*2.07*	*0.33*
G	*1100*	*60.25*	*3.534*	*199.6*	*22.7*	*0.14*	*2.6*	*89.7*	*3.30*	*0.57*
H	*1275*	*48.60*	*13.36*	*160.5*	*35.2*	*0.038*	*4.7*	*98.7*	*4.87*	*0.47*
I	*1725*	*63.04*	*17.40*	*209.8*	*5.09*	*0.029*	*3.9*	*100.0*	*5.30*	*0.69*
Integrated age ± 2σ			n=9		390.8				7.12	1.75
Plateau ± 2σ	steps B-E		n=4	MSWD=4.39	275.2	0.27		70.4	1.33	0.45
Isochron±2σ	steps A-I		n=9	MSWD = 8.9	$^{40}Ar/^{36}Ar$=304.4±5.4				0.08	0.06
VY9503-1, Groundmass Concentrate, J=0.0010592±0.18%, D=1.0063±0.001, NM-182J, Lab#=55176-01										
A	*650*	*1943.6*	*1.059*	*6343.4*	*15.1*	*0.48*	*3.6*	*3.4*	*127.67*	*16.58*
B	*725*	*73.94*	*0.7095*	*241.6*	*45.7*	*0.72*	*3.5*	*13.6*	*4.95*	*0.57*
C	775	36.93	0.7987	121.5	10.8	0.64	2.9	16.0	2.07	0.37
D	825	25.27	1.244	81.87	110.1	0.41	4.7	40.5	2.26	0.20
E	900	13.79	1.278	44.19	83.3	0.40	6.1	59.1	1.60	0.11
F	1000	19.47	1.729	63.81	78.2	0.30	3.9	76.5	1.44	0.16
G	*1100*	*35.04*	*1.899*	*113.8*	*41.7*	*0.27*	*4.5*	*85.8*	*3.03*	*0.31*
H	*1275*	*75.83*	*7.301*	*251.9*	*42.4*	*0.070*	*2.6*	*95.2*	*3.83*	*0.62*
I	*1725*	*67.07*	*10.89*	*220.6*	*21.5*	*0.047*	*4.2*	*100.0*	*5.35*	*0.55*
Integrated age ± 2σ			n=9		448.8				7.01	1.63
Plateau ± 2σ	steps C-F		n=4	MSWD=3.98	282.3	0.38		62.9	1.69	0.33
Isochron±2σ	steps A-I		n=9	MSWD = 2.7	$^{40}Ar/^{36}Ar$=304.7±2.6				0.68	0.33

ID	Power (°C)	$^{40}Ar/^{39}Ar$	$^{37}Ar/^{39}Ar$	$^{36}Ar/^{39}Ar$ (x 10^{-3})	$^{39}Ar_K$ (x 10^{-15} mol)	K/Ca	$^{40}Ar^*$ (%)	^{39}Ar (%)	Age (Ma)	±1σ (Ma)
JP-3, Groundmass Concentrate, J=0.0010409±0.27%, D=1.0063±0.001, NM-182K, Lab#=55183-01										
A	*625*	*1926.9*	*0.9139*	*6383.3*	*2.86*	*0.56*	*2.1*	*0.9*	*74.90*	*14.49*
B	*700*	*26.97*	*0.9204*	*43.71*	*10.5*	*0.55*	*52.4*	*4.3*	*26.35*	*0.19*
C	*750*	*16.69*	*0.7869*	*8.299*	*10.6*	*0.65*	*85.7*	*7.8*	*26.68*	*0.13*
D	*800*	*15.29*	*0.6150*	*3.942*	*23.7*	*0.83*	*92.7*	*15.5*	*26.44*	*0.06*
E	*875*	*14.75*	*0.4733*	*2.755*	*54.5*	*1.1*	*94.7*	*33.3*	*26.07*	*0.05*
F	975	14.85	0.3981	3.431	73.4	1.3	93.4	57.3	25.86	0.05
G	1075	16.48	0.3837	9.189	60.0	1.3	83.7	76.8	25.74	0.06
H	1250	18.74	0.9871	16.50	47.2	0.52	74.4	92.2	26.01	0.10
I	1700	21.00	2.230	24.32	23.8	0.23	66.7	100.0	26.14	0.13
Integrated age ± 2σ			n=9		306.4				26.47	0.40
Plateau ± 2σ	steps F-I		n=4	MSWD=3.69	204.3	1.00		66.7	25.86	0.19

Isotopic ratios corrected for blank, radioactive decay, and mass discrimination, not corrected for interfering reactions.
Ages calculated relative to FC-1 Fish Canyon Tuff sanidine interlaboratory standard at 28.02 Ma.
Errors quoted for individual analyses include analytical error only, without interfering reaction or J uncertainties.
Integrated age calculated by recombining isotopic measurements of all steps.
Integrated age error calculated by recombining errors of isotopic measurements of all steps.
Plateau age is inverse-variance-weighted mean of selected steps.
Plateau age error is inverse-variance-weighted mean error (Taylor, 1982) times root MSWD where MSWD>1.
Plateau and integrated ages incorporate uncertainties in interferring reaction corrections and J factors.
Decay constants and isotopic abundances after Steiger and Jaeger (1977).
# symbol preceding sample ID denotes analyses excluded from plateau age calculations.
Discrimination = 1.0063 ± 0.001
Correction factors:
$(^{39}Ar/^{37}Ar)_{Ca}$ = 0.0007 ± 5e-05
$(^{36}Ar/^{37}Ar)_{Ca}$ = 0.00028 ± 1e-05
$(^{38}Ar/^{39}Ar)_{K}$ = 0.0133
$(^{40}Ar/^{39}Ar)_{K}$ = 0 ± 0.0004

New Mexico Bureau of Mines and Mineral Resources

Procedures of the New Mexico Geochronology Research Laboratory

For the Period June 1998 – present

Matthew Heizler
William C. McIntosh
Richard Esser
Lisa Peters

$^{40}Ar/^{39}Ar$ and K-Ar dating

Often, large bulk samples (either minerals or whole rocks) are required for K-Ar dating and even small amounts of xenocrystic, authigenic, or other non-ideal behavior can lead to inaccuracy. The K-Ar technique is susceptible to sample inhomogeneity as separate aliquots are required for the potassium and argon determinations. The need to determine absolute quantities (i.e. moles of $^{40}Ar^*$ and ^{40}K) limits the precision of the K-Ar method to approximately 1% and also, the technique provides limited potential to evaluate underlying assumptions. In the $^{40}Ar/^{39}Ar$ variant of the K-Ar technique, a sample is irradiated with fast neutrons thereby converting ^{39}K to ^{39}Ar through a (n,p) reaction. Following irradiation, the sample is either fused or incrementally heated and the gas analyzed in the same manner as in the conventional K-Ar procedure, with one exception, no argon spike need be added.

Some of the advantages of the $^{40}Ar/^{39}Ar$ method over the conventional K-Ar technique are:

1. A single analysis is conducted on one aliquot of sample thereby reducing the sample size and eliminating sample inhomogeneity.
2. Analytical error incurred in determining absolute abundances is reduced by measuring only isotopic ratios. This also eliminates the need to know the exact weight of the sample.
3. The addition of an argon spike is not necessary.
4. The sample does not need to be completely fused, but rather can be incrementally heated. The $^{40}Ar/^{39}Ar$ ratio (age) can be measured for each fraction of argon released and this allows for the generation of an age spectrum.

The age of a sample as determined with the $^{40}Ar/^{39}Ar$ method requires comparison of the measured $^{40}Ar/^{39}Ar$ ratio with that of a standard of known age. Also, several isotopes of other elements (Ca, K, Cl, Ar) produce argon during the irradiation procedure and must be corrected for. Far more in-depth details of the determination of an apparent age via the $^{40}Ar/^{39}Ar$ method are given in Dalrymple et al. (1981) and McDougall and Harrison (1988).

Analytical techniques

Sample Preparation and irradiation details

Mineral separates are obtained in various fashions depending upon the mineral of interest, rock type and grain size. In almost all cases the sample is crushed in a jaw crusher and ground in a disc grinder and then sized. The size fraction used generally corresponds to the largest size possible which will permit obtaining a pure mineral separate. Following sizing, the sample is washed and dried. For plutonic and metamorphic rocks and lavas, crystals are separated using standard heavy liquid, Franz magnetic and hand-picking techniques. For volcanic sanidine and plagioclase, the sized sample is reacted with 15% HF acid to remove glass and/or matrix and then thoroughly washed prior to heavy liquid and magnetic separation. For groundmass concentrates, rock fragments are selected which do not contain any visible phenocrysts.

The NMGRL uses either the Ford reactor at the University of Michigan or the Nuclear Science Center reactor at Texas A&M University. At the Ford reactor, the L67 position is used (unless otherwise noted) and the D-3 position is always used at the Texas A&M reactor. All of the Michigan irradiations are carried out underwater without any shielding for thermal neutrons, whereas the Texas irradiations are in a dry location which is shielded with B and Cd. Depending upon the reactor used, the mineral separates are loaded into either holes drilled into Al discs or into 6 mm I.D. quartz tubes. Various Al discs are used. For Michigan, either six hole or twelve hole, 1 cm diameter discs are used and all holes are of equal size. Samples are placed in the 0, 120 and 240° locations and standards in the 60, 180 and 300° locations for the six hole disc. For the twelve hole disc, samples are located at 30, 60, 120, 150, 210, 240, 300, and 330° and standards at 0, 90, 180 and 270 degrees. If samples are loaded into the quartz tubes, they are wrapped in Cu foil with standards interleaved at ~0.5 cm intervals. For Texas, 2.4 cm diameter discs contain either sixteen or six sample holes with smaller holes used to hold the standards. For the six hole disc, sample locations are 30, 90, 150, 210, 270 and 330° and standards are at 0, 60, 120, 180, 240 and 300°. Samples are located at 18, 36, 54, 72, 108, 126, 144, 162, 198, 216, 234, 252, 288, 306, 324, 342 degrees and standards at 0, 90, 180 and 270 degrees in the sixteen hole disc. Following sample loading into the discs, the discs are stacked, screwed together and sealed

in vacuo in either quartz (Michigan) or Pyrex (Texas) tubes.

Extraction Line and Mass Spectrometer details

The NMGRL argon extraction line has both a double vacuum Mo resistance furnace and a CO_2 laser to heat samples. The Mo furnace crucible is heated with a W heating element and the temperature is monitored with a W-Re thermocouple placed in a hole drilled into the bottom of the crucible. A one inch long Mo liner is placed in the bottom of the crucible to collect the melted samples. The furnace temperature is calibrated by either/or melting Cu foil or with an additional thermocouple inserted in the top of the furnace down to the liner. The CO_2 laser is a Synrad 10W laser equipped with a He-Ne pointing laser. The laser chamber is constructed from a 3 3/8" stainless steel conflat and the window material is ZnS. The extraction line is a two stage design. The first stage is equipped with a SAES GP-50 getter, whereas the second stage houses two SAES GP-50 getters and a tungsten filament. The first stage getter is operated at 450°C as is one of the second stage getters. The other second stage getter is operated at room temperature and the tungsten filament is operated at ~2000°C. Gases evolved from samples heated in the furnace are reacted with the first stage getter during heating. Following heating, the gas is expanded into the second stage for two minutes and then isolated from the first stage. During second stage cleaning, the first stage and furnace are pumped out. After gettering in the second stage, the gas is expanded into the mass spectrometer. Gases evolved from samples heated in the laser are expanded through a cold finger operated at -140°C and directly into the second stage. Following cleanup, the gas in the second stage and laser chamber is expanded into the mass spectrometer for analysis.

The NMGRL employs a MAP-215-50 mass spectrometer which is operated in static mode. The mass spectrometer is operated with a resolution ranging between 450 to 600 at mass 40 and isotopes are detected on a Johnston electron multiplier operated at ~2.1 kV with an overall gain of about 10,000 over the Faraday collector. Final isotopic intensities are determined by linear regression to time zero of the peak height versus time following gas introduction for each mass. Each mass intensity is corrected for mass spectrometer baseline and background and the extraction system blank.

Blanks for the furnace are generally determined at the beginning of a run while the furnace is cold and then between heating steps while the furnace is cooling. Typically, a blank is

run every three to six heating steps. Periodic furnace hot blank analysis reveals that the cold blank is equivalent to the hot blank for temperatures less than about 1300°C. Laser system blanks are generally determined between every four analyses. Mass discrimination is measured using atmospheric argon which has been dried using a Ti-sublimation pump. Typically, 10 to 15 replicate air analyses are measured to determine a mean mass discrimination value. Air pipette analyses are generally conducted 2-3 times per month, but more often when samples sensitive to the mass discrimination value are analyzed. Correction factors for interfering nuclear reactions on K and Ca are determined using K-glass and CaF_2, respectively. Typically, 3-5 individual pieces of the salt or glass are fused with the CO_2 laser and the correction factors are calculated from the weighted mean of the individual determinations.

Data acquisition, presentation and age calculation

Samples are either step-heated or fused in a single increment (total fusion). Bulk samples are often step-heated and the data are generally displayed on an age spectrum or isochron diagram. Single crystals are often analyzed by the total fusion method and the results are typically displayed on probability distribution diagrams or isochron diagrams.

The Age Spectrum Diagram

Age spectra plot apparent age of each incrementally heated gas fraction versus the cumulative % $^{39}Ar_K$ released, with steps increasing in temperature from left to right. Each apparent age is calculated assuming that the trapped argon (argon not produced by *in situ* decay of ^{40}K) has the modern day atmospheric $^{40}Ar/^{36}Ar$ value of 295.5. Additional parameters for each heating step are often plotted versus the cumulative $\%^{39}Ar_K$ released. These auxiliary parameters can aid age spectra interpretation and may include radiogenic yield (percent of ^{40}Ar which is not atmospheric), K/Ca (determined from measured Ca-derived ^{37}Ar and K-derived ^{39}Ar) and/or K/Cl (determined from measured Cl-derived ^{38}Ar and K-derived ^{39}Ar). Incremental heating analysis is often effective at revealing complex argon systematics related to excess argon, alteration, contamination, ^{39}Ar recoil, argon loss, etc. Often low-temperature heating steps have low radiogenic yields and apparent ages with relatively high errors due mainly to

loosely held, non-radiogenic argon residing on grain surfaces or along grain boundaries. An entirely or partially flat spectrum, in which apparent ages are the same within analytical error, may indicate that the sample is homogeneous with respect to K and Ar and has had a simple thermal and geological history. A drawback to the age spectrum technique is encountered when hydrous minerals such as micas and amphiboles are analyzed. These minerals are not stable in the ultra-high vacuum extraction system and thus step-heating can homogenize important details of the true ^{40}Ar distribution. In other words, a flat age spectrum may result even if a hydrous sample has a complex argon distribution.

The Isochron Diagram

Argon data can be plotted on isotope correlation diagrams to help assess the isotopic composition of Ar trapped at the time of argon closure, thereby testing the assumption that trapped argon isotopes have the composition of modern atmosphere which is implicit in age spectra. To construct an "inverse isochron" the $^{36}Ar/^{40}Ar$ ratio is plotted versus the $^{39}Ar/^{40}Ar$ ratio. A best fit line can be calculated for the data array which yields the value for the trapped argon (Y-axis intercept) and the $^{40}Ar^*/^{39}Ar_K$ value (age) from the X-axis intercept. Isochron analysis is most useful for step-heated or total fusion data which have a significant spread in radiogenic yield. For young or low K samples, the calculated apparent age can be very sensitive to the composition of the trapped argon and therefore isochron analysis should be preformed routinely on these samples (cf. Heizler and Harrison, 1988). For very old (>Mesozoic) samples or relatively old sanidines (>mid-Cenozoic) the data are often highly radiogenic and cluster near the X-axis thereby making isochron analysis of little value.

The Probability Distribution Diagram

The probability distribution diagram, which is sometimes referred to as an ideogram, is a plot of apparent age versus the summation of the normal distribution of each individual analysis (Deino and Potts, 1992). This diagram is most effective at displaying single crystal laser fusion data to assess the distribution of the population. The K/Ca, radiogenic yield, and the moles of ^{39}Ar for each analysis are also often displayed for each sample as this allows for visual ease in identifying apparent age correlations between, for instance, plagioclase contamination, signal size and/or radiogenic concentrations. The error (1σ) for each age analysis is generally shown by the horizontal lines in the moles of ^{39}Ar section. Solid symbols represent the analyses used for the weighted mean age calculation and the generation of the solid line on the ideogram, whereas open symbols represent data omitted from the age calculation. If shown, a dashed line represents the probability distribution of all of the displayed data. The diagram is most effective for displaying the form of the age distribution (i.e. gaussian, skewed, etc.) and for identifying xenocrystic or other grains which fall outside of the main population.

Error Calculations

For step-heated samples, a plateau for the age spectrum is defined by the steps indicated. The plateau age is calculated by weighting each step on the plateau by the inverse of the variance and the error is calculated by either the method of Samson and Alexander (1987) or Taylor (1982). A mean sum weighted deviates (MSWD) value is determined by dividing the Chi-squared value by n-1 degrees of freedom for the plateau ages. If the MSWD value is outside the 95% confidence window (cf. Mahon, 1996; Table 1), the plateau or preferred age error is multiplied by the square root of the MSWD.

For single crystal fusion data, a weighted mean is calculated using the inverse of the variance to weight each age determination (Taylor, 1982). Errors are calculated as described for the plateau ages above.

Isochron ages, $^{40}Ar/^{36}Ar_i$ values and MSWD values are calculated from the regression results obtained by the York (1969) method.

References cited

Dalrymple, G.B., Alexander, E.C., Jr., Lanphere, M.A., and Kraker, G.P., 1981. Irradiation of samples for $^{40}Ar/^{39}Ar$ dating using the Geological Survey TRIGA reactor. U.S.G.S., Prof. Paper, 1176.

Deino, A., and Potts, R., 1990. Single-Crystal $^{40}Ar/^{39}Ar$ dating of the Olorgesailie Formation, Southern Kenya Rift, J. Geophys. Res., 95, 8453-8470.

Deino, A., and Potts, R., 1992. Age-probability spectra from examination of single-crystal $^{40}Ar/^{39}Ar$ dating results: Examples from Olorgesailie, Southern Kenya Rift, Quat. International, 13/14, 47-53.

Fleck, R.J., Sutter, J.F., and Elliot, D.H., 1977. Interpretation of discordant $^{40}Ar/^{39}Ar$ age-spectra of Mesozoic tholieiites from Antarctica, Geochim. Cosmochim. Acta, 41, 15-32.

Heizler, M. T., and Harrison, T. M., 1988. Multiple trapped argon components revealed by $^{40}Ar/^{39}Ar$ analysis, Geochim. Cosmochim. Acta, 52, 295-1303.

Mahon, K.I., 1996. The New "York" regression: Application of an improved statistical method to geochemistry, International Geology Review, 38, 293-303.

McDougall, I., and Harrison, T.M., 1988. Geochronology and thermochronology by the ^{40}Ar-^{39}Ar method. Oxford University Press.

Samson, S.D., and, Alexander, E.C., Jr., 1987. Calibration of the interlaboratory $^{40}Ar/^{39}Ar$ dating standard, Mmhb-1, Chem. Geol., 66, 27-34.

Steiger, R.H., and Jäger, E., 1977. Subcommission on geochronology: Convention on the use of decay constants in geo- and cosmochronology. Earth and Planet. Sci. Lett., 36, 359-362.

Taylor, J.R., 1982. An Introduction to Error Analysis: The Study of Uncertainties in Physical Measurements,. Univ. Sci. Books, Mill Valley, Calif., 270 p.

York, D., 1969. Least squares fitting of a straight line with correlated errors, Earth and Planet. Sci. Lett.., 5, 320-324.